COHERENCE OF LIGHT-MATTER INTERACTION

LEE JONG WEY

A project report submitted in partial fulfilment of the requirements for the award of Bachelor of Science (Hons.) Physics

Lee Kong Chian Faculty of Engineering and Science
Universiti Tunku Abdul Rahman

August 2017

DECLARATION

I hereby declare that this project report is based on my original work except for citations and quotations which have been duly acknowledged. I also declare that it has not been previously and concurrently submitted for any other degree or award at UTAR or other institutions.

Signature : _____

Name : LEE JONG WEY

ID No. : 14UEB07357

Date : _____

APPROVAL FOR SUBMISSION

I certify that this project report entitled **"COHERENCE OF LIGHT-MATTER INTERACTION"** was prepared by **LEE JONG WEY** has met the required standard for submission in partial fulfilment of the requirements for the award of Bachelor of Science (Hons.) Physics at Universiti Tunku Abdul Rahman.

Approved by,

Signature : _____

Supervisor : DR TAN ENG KIANG

Date : _____

ABSTRACT

This thesis reports on semiclassical and full quantum mechanical treatments of light-matter interaction. In particular, we look at the interaction between single-mode light field and a two-level atom in a non-dissipating closed system. In semiclassical treatment, the interaction is dominated by electric-dipole interaction, thus the electric-dipole Hamiltonian is formulated in which, together with the atomic Hamiltonian, forms the total Hamiltonian of the system. Derivations to obtain the probability function of the atom in ground state and excited state are performed. Two cases of detuning, namely exact resonance and near resonance are then studied. In exact resonance, it is found that the probability of the atom to reside in ground state and excited state is conserved and varied in sinusoidal waveform. In the case of near resonant, the period and the amplitude of the probability function decreases with higher detuning. On the other hand, in full quantum mechanical treatment, we consider quantised light field of various initial field states interacting with a quantum mechanical two-level atom. The total Hamiltonian of the system consists of atomic Hamiltonian, field Hamiltonian and interaction Hamiltonian is derived, which is then transformed into the interaction picture. The derived Hamiltonian is then used to solve the Schrodinger equation to find the wavefunction of the joint system. Finally, initial field states such as number state, coherent state and thermal state are used to obtain the ground state probability functions of the two-level system. Initial number state renders the atom to undergo a uniform oscillation in probability function, similar as in the case of the semiclassical treatment. Initial thermal field interacting with the atom turns the probability function to exhibit chaotic characteristics, resulting in minimal amount of information to be extracted from the system. Most interestingly, initial coherent state condition allows for the observation of the collapse and revival of Rabi oscillation. Such phenomenon is a characteristic feature of the quantum mechanical treatment and in fact, is the direct evidence of the quantisation of the field state. The time period between each revival features is also investigated and is found that the period is related to mean photon number and interaction strength by the formula $T \approx 2\pi\, \lambda^{-1}\sqrt{\bar{n}}$. Furthermore, the derived model is extended from single-photon model to multiple-photon model in which the two-level atom absorbs multiple photons to undergo excitation. In the case of two-photon model with initial coherent state, we observe collapse and revival features with much

shorter period. The probability function with initial thermal state, on the other hand, remains chaotic even in two-photon model.

TABLE OF CONTENTS

LIST OF TABLES

LIST OF FIGURES

LIST OF APPENDICES

CHAPTER 1

INTRODUCTION

1.1 Background

Much of the interests in studying the interaction of light with matter have been generated over the past few centuries. Traditional studies on such interaction involve classical treatment of light as an electromagnetic wave and atom as a Hertzian dipole. Interactions can be observed when the oscillation of electromagnetic wave is in resonant with the dipole. Besides that, the interaction of light with media may also be in the form of absorption, transmission, reflection and scattering.

In the advent of quantum mechanics, quantum optics is introduced which involves the semiclassical and quantum mechanical treatments of light-matter interaction. In quantum mechanics, the energy levels of the atom are quantised as opposed to continuous in classical theories. Semiclassical treatment requires such quantum mechanical atom, but still retains the classical properties of the light field.

To completely investigate the light-matter interaction, a full quantum mechanical treatment is applied to both the atom and the light field. In this treatment, the light is quantised and is considered as photons. One important model of this treatment is the Jaynes-Cummings model which was introduced by Edwin Jaynes and Fred Cummings in 1963. This model was first used to investigate the classical aspect of spontaneous emission, but later found that their work resulted in showing the discreteness of the photons.

1.2 Problem Statement and Importance of the Study

Quantum applications have seen rapid development over the last few decades. One of the earliest progresses was in 1917 when Einstein developed the theoretical foundations of laser and maser. However it was not until in the year 1939 that Lamb and Rutherford first demonstrated the stimulated emission process. A few years later Kastler and Weber proposed light and microwave amplification respectively, which later became the experimental foundation for laser and maser. These developments stimulated a new field of quantum electronics. Besides that, photonic qubits remain as one of the main candidates for quantum computing and long-distance quantum teleportation.

All these aforementioned developments require the interactions between light and matter. Therefore a solid understanding on the nature of such interaction is required in order to analyse the theories behind these recent progresses as well as possible future applications.

1.3 Aims and Objectives of the Study

Given the importance of quantum optics in the modern research and development, this study aims to investigate the fundamental problem of light-matter interaction using both semiclassical and quantum mechanical treatments. In semiclassical treatment, the probabilities of the two-level system to reside in either ground state or excited state is derived and discussed. This report also aims to highlight the mathematical procedure in obtaining the theoretical form of the interaction between an energetically quantised two-level atom and a classical light field.

Besides that, it is also one of this project's main objectives to perform quantum mechanical treatment on the interaction between a two-level atom and various single-mode quantised light sources. The characteristic features of these light-matter interactions will be studied thoroughly. This study also aims to demonstrate the mathematical derivation of wavefunction of the interaction system. Furthermore, in-depth studies on the properties of the collapse and revival features of the Rabi oscillations are performed.

1.4 Scope and Limitations of the Study

This thesis reports primarily on the interaction between a single-mode light field and a two-level atom in a non-dissipative closed system. The scope of this study can be generally classified into two types, semiclassical and quantum mechanical treatments. In semiclassical treatment, the energy level of the atom is assumed to be quantised whereas the field is of classical nature. On the other hand, quantum mechanical treatment assumed energetically quantised two-level atom and quantised light field statistics.

The study, however, is limited to closed system in which decoherence and energy dissipation do not occur. Several approximations such as rotating-wave approximation and dipole approximation are also utilised in the derivations. A thorough study without the use of these approximations is beyond the scope of this project.

1.5 Outline of the study

The study begins with a complete investigation on the semiclassical treatment of light-matter interaction. To simplify the scenario, several approximations such as dipole approximation and rotating-wave approximation are utilised. From the derived results, the probabilities of the atom to be found in either ground state or excited state are computed and discussed.

Then, derivations on the quantum mechanical treatment of interaction between a two-level atom and various single-modes quantised field states are performed. For the purpose of this study, Jaynes-Cummings Model was chosen to develop the wavefunction of the light-matter system. To achieve that, the quantisation of electromagnetic field, which is assumed to be a free field contained inside a closed resonator with perfectly conducting walls, is derived and reported. Various properties of quantum fields such as number states, coherent states and thermal states are investigated as well. After obtaining the wavefunction of the interacting system, the probability graphs of the atom staying in the ground state are plotted and studied for various conditions such as resonant and near resonant cases. Furthermore, an in-depth study on the properties of the collapse and revival features of the Rabi oscillations is performed.

CHAPTER 2

LITERATURE REVIEW

2.1 Dipole Interaction with External Electric field

In semiclassical treatment, the interaction Hamiltonian between a two-level atom and a classical field needs to be derived. There are commonly two starting points: a minimal coupling Hamiltonian and a direct coupling Hamiltonian (Rzazewski and Boyd, 2004). These methods are also known as velocity gauge and length gauge respectively. According to Dick (2016), although the two gauges may come into different results for atoms in strong fields, it is still mathematically consistent to mix some components of the two gauges. However, since quantum mechanics is generally gauge invariant, the choice of the formulation should not affect the final result considerably (Han and Madsen, 2010). Hence in this report, the direct coupling Hamiltonian is chosen to formulate the interaction Hamiltonian because it is conceptually simpler. The derivation for such formulation is shown in this section.

According to Griffith (1999), a dipole may interact with a uniform or non-uniform electric field. Suppose a perfect dipole is located inside an electric field as shown in figure 2.1, it experiences a force

$$\begin{aligned} \boldsymbol{F} &= q(\boldsymbol{E}_+ - \boldsymbol{E}_-) \\ &= \boldsymbol{F}_+ + \boldsymbol{F}_- , \end{aligned}$$

where $\boldsymbol{F}_+ = q\boldsymbol{E}_+$ and $\boldsymbol{F}_- = -q\boldsymbol{E}_-$. The electric fields $\boldsymbol{E}_+$ and $\boldsymbol{E}_-$ are the fields that interact with $+q$ charge and $-q$ charge respectively. In a uniform field, the force in the positive direction $\boldsymbol{F}_+$ and the force in the negative direction $\boldsymbol{F}_-$ cancel each other completely, leaving no net force acting on the dipole. There will be however a torque such that

$$\begin{aligned} \boldsymbol{N} &= (\boldsymbol{r}_+ \times \boldsymbol{F}_+) + (\boldsymbol{r}_- \times \boldsymbol{F}_-) \\ &= \left(\frac{\boldsymbol{r}'}{2} \times q\boldsymbol{E}\right) + \left(-\frac{\boldsymbol{r}'}{2} \times -q\boldsymbol{E}\right) \\ &= q\boldsymbol{r}' \times \boldsymbol{E} \\ &= \boldsymbol{d} \times \boldsymbol{E} , \end{aligned}$$

where $\boldsymbol{d} = q\boldsymbol{r}'$ is the dipole moment and $\boldsymbol{r}'$ is the position vector of the charges.

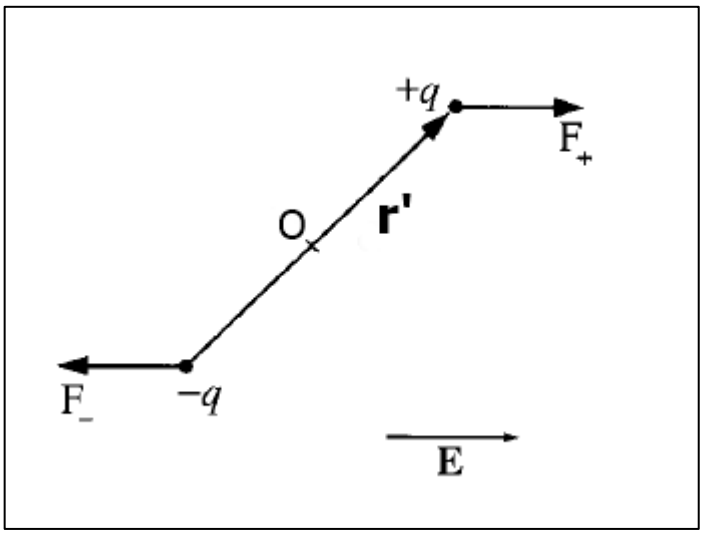

Figure 2.1: Schematic drawing of a dipole located inside an electric field.

On the contrary, a non-uniform electric field does inflict a net force on the dipole because $\boldsymbol{F}_+$ and $\boldsymbol{F}_-$ do not exactly cancel each other. The force experienced by the dipole is again given by

$$\begin{aligned} \boldsymbol{F} &= q(\boldsymbol{E}_+ - \boldsymbol{E}_-) \\ &= q(\Delta \boldsymbol{E}) , \end{aligned} \tag{2.1}$$

where $\Delta\boldsymbol{E}$ is the difference between the $\boldsymbol{E}$ field at the $+q$ charge and the $-q$ charge. Now if we assume that the dipole is very short, the small change in the $\boldsymbol{E}$ field can be approximated as $\Delta\boldsymbol{E} = (\boldsymbol{r}' \cdot \boldsymbol{\nabla})\boldsymbol{E}$ which can then be substituted back into equation 2.1 so that

$$\boldsymbol{F} = (\boldsymbol{d} \cdot \nabla)\boldsymbol{E}.$$

In addition to that, the dipole in a non-uniform field also experiences a torque which is the same as the torque experienced by the dipole in a uniform field.

To find the energy of an ideal dipole in an electric field, the work done on the point charge $-q$ and $+q$ are recognised to be $W = -qV(\boldsymbol{r})$ and $W = qV(\boldsymbol{r} + \boldsymbol{r}')$

respectively. The vector $\boldsymbol{r}$ describes the position of the $-q$ charge measured from an arbitrary origin. The energy of the dipole is then given by

$$\begin{aligned} U &= qV(\boldsymbol{r}+\boldsymbol{r}') - qV(\boldsymbol{r}) \\ &= q[V(\boldsymbol{r}+\boldsymbol{r}') - V(\boldsymbol{r})] \\ &= q\left[-\int_{\boldsymbol{r}}^{r+r'} E \cdot dl\right]. \end{aligned}$$

For an ideal dipole, the energy can be simplified into

$$U = -q\boldsymbol{E}\cdot\boldsymbol{r}' = -\boldsymbol{d}\cdot\boldsymbol{E}\,,$$

which can be extended as a direct coupling Hamiltonian taking the form

$$\widehat{H}_{ED} = -\widehat{\boldsymbol{d}}\cdot\boldsymbol{E}\,, \tag{2.2}$$

where $\widehat{H}_{ED}$ represents electric-dipole Hamiltonian operator and $\widehat{\boldsymbol{d}}$ is a dipole operator.

2.2 Quantum Harmonic Oscillator

The solution of a quantum harmonic oscillator remains relevant in quantum optics because the quantisation of electromagnetic field yields similar result as a harmonic oscillator, hence this part of the literature is included. For simplicity, the harmonic oscillator is taken to be one-dimensional, however the solution may be generalised into higher dimensional oscillator. Firstly, the potential of a harmonic oscillator is written as $V(x) = \frac{1}{2}m\omega^2x^2$, which can then be substituted into the Schrodinger equation so that

$$i\hbar\frac{\partial\Psi}{\partial t} = -\frac{\hbar^2}{2m}\frac{\partial^2\Psi}{\partial x^2} + \frac{1}{2}m\omega^2x^2\Psi\,.$$

Since the potential is time independent, the wavefunction Ψ may take the form of separable solution where $\Psi(x,t) = \psi(x)\phi(t)$. Since the left side of the equation only depends on time whereas the right side of the equation only depends on position,

the two sides must be equal to a certain constant. Let that constant be energy, E and separate the equation, we therefore obtain

$$i\hbar\frac{\partial\phi}{\partial t} = E\phi\ ,$$

and

$$-\frac{\hbar^2}{2m}\frac{\partial^2\psi}{\partial x^2} + \frac{1}{2}m\omega^2\hat{x}^2\psi = \mathrm{E}\psi\ .$$

The solution of the time dependent part of the equation is simply

$$\phi(t) = \exp\left(-\frac{iEt}{\hbar}\right).$$

On the other hand, the spatial part of the equation can be rewritten as

$$\frac{1}{2m}[\hat{p}^2 + (m\omega\hat{x})^2]\psi = E\psi\ .$$

Since $\hat{H}\psi = E\psi$, then the Hamiltonian operator is

$$\hat{H} = \frac{1}{2m}[\hat{p}^2 + (m\omega\hat{x})^2]\ .$$

To obtain the solution using algebraic method, we define the ladder operators as

$$\hat{a}_{\pm} = \frac{1}{\sqrt{2\hbar m\omega}}(\mp i\hat{p} + m\omega\hat{x}), \tag{2.3}$$

where $\hat{a}_{+}$ is a step up operator and $\hat{a}_{-}$ is a step down operator. The product of these two operators yields

$$\hat{a}_{+}\hat{a}_{-} = \frac{1}{2\hbar m\omega}[\hat{p}^2 + (m\omega\hat{x})^2 + im\omega(\hat{p}\hat{x} - \hat{x}\hat{p})]. \tag{2.4}$$

Since the $\hat{x}$ operator and $\hat{p}$ operator do not commute, the term $-\frac{1}{2\hbar m\omega}[im\omega(\hat{p}\hat{x} - \hat{x}\hat{p})]$ remains non-zero. To simplify the extra term, the commutator of these two operators using a test function f is found to be:

$$\begin{aligned}\hat{p}\hat{x} - \hat{x}\hat{p} &= [\hat{p}, \hat{x}]f \\ &= \frac{\hbar}{i}\frac{d}{dx}xf - \frac{x\hbar}{i}\frac{d}{dx}f \\ &= \frac{\hbar}{i}\left(x\frac{df}{dx} + f - x\frac{df}{dx}\right) \\ &= -i\hbar f\ .\end{aligned}$$

$$\therefore\ [\hat{p}, \hat{x}] = -i\hbar\ .$$

The extra term then simplifies into $-\frac{m\omega\hbar}{2\hbar m\omega} = -\frac{1}{2}$. In other words the Hamiltonian simplifies into

$$\begin{aligned}\widehat{H} &= \hbar\omega\left(\hat{a}_+\hat{a}_- + \tfrac{1}{2}\right) \\ &= \hbar\omega\left(\hat{n} + \frac{1}{2}\right),\end{aligned} \tag{2.5}$$

where $\hat{n} = \hat{a}_+\hat{a}_-$ is a number operator with eigenstates of $|n\rangle$ and corresponding eigenvalues of n. It therefore follows the relation

$$\hat{n}|n\rangle = n|n\rangle.$$

The time-independent Schrodinger equation simplifies into

$$\hbar\omega\left(\hat{a}_+\hat{a}_- + \frac{1}{2}\right)\psi = E\psi.$$

It is also useful to note a few properties of the ladder operators as follows:

$$[\hat{a}_-, \hat{a}_+] = 1, \tag{2.6}$$

$$\hat{a}_+|n\rangle = \sqrt{n+1}|n+1\rangle, \tag{2.7}$$

$$\hat{a}_-|n\rangle = \sqrt{n}|n-1\rangle, \tag{2.8}$$

$$\hat{H}(\hat{a}_+\psi) = (E+\hbar\omega)(\hat{a}_+\psi), \tag{2.9}$$

$$\hat{H}(\hat{a}_-\psi) = (E-\hbar\omega)(\hat{a}_-\psi). \tag{2.10}$$

The observable operators can be expressed in terms of the ladder operators as well, i.e.

$$\hat{x} = \sqrt{\frac{\hbar}{2m\omega}}(\hat{a}_+ + \hat{a}_-) \tag{2.11}$$

and

$$\hat{p} = i\sqrt{\frac{\hbar m\omega}{2}}(\hat{a}_+ - \hat{a}_-). \tag{2.12}$$

2.3 Quantisation of Electromagnetic Field

Majority of the works in this section were derived based on the methods shown by Loudon (2000) and Schleich (2001). The electromagnetic field to be quantised in this section is modelled as a free field trapped inside a resonator in which the walls are made of perfect conductors. While the classical fields are shown to have quantised properties for having spatial modes, the quantisation procedure in this section is focused more on the quantisation of the temporal part of the vector potential. We begin by describing the classical electromagnetic field using Maxwell's four equations as shown below:

$$\boldsymbol{\nabla}\times\boldsymbol{E} = -\frac{\partial \boldsymbol{B}}{\partial t}, \tag{2.13}$$

$$\mu_0{}^{-1}\boldsymbol{\nabla}\times\boldsymbol{B} = \varepsilon_0\frac{\partial \boldsymbol{E}}{\partial t} + \boldsymbol{J}, \tag{2.14}$$

$$\varepsilon_0\boldsymbol{\nabla}\cdot\boldsymbol{E} = \rho, \tag{2.15}$$

$$\boldsymbol{\nabla}\cdot\boldsymbol{B} = 0. \tag{2.16}$$

The variables $\boldsymbol{J}$ and ρ are current density and charge density respectively. These classical fields are functions of position $\boldsymbol{r}$ and time t. The quantisation of electromagnetic field can be facilitated by re-expressing the Maxwell equation in terms of scalar potential ϕ and vector potential $\boldsymbol{A}$.

2.3.1 Wave Equations of the Potentials

Firstly, it can be immediately seen that to satisfy equation 2.16, the $\boldsymbol{B}$ field can be expressed as

$$\boldsymbol{B} = \boldsymbol{\nabla}\times\boldsymbol{A}. \tag{2.17}$$

Substitute equation 2.17 into equation 2.13 and simplify it using the identity $\boldsymbol{\nabla}\times\boldsymbol{\nabla}\phi = 0$, we obtain

$$-\boldsymbol{\nabla}\times\boldsymbol{E} - \boldsymbol{\nabla}\times\frac{\partial \boldsymbol{A}}{\partial t} = 0 = \boldsymbol{\nabla}\times\boldsymbol{\nabla}\phi$$

$$\boldsymbol{\nabla}\times\boldsymbol{\nabla}\phi = \boldsymbol{\nabla}\times\left(-\boldsymbol{E} - \frac{\partial \boldsymbol{A}}{\partial t}\right)$$

$$\boldsymbol{\nabla}\phi = \left(-\boldsymbol{E} - \frac{\partial \boldsymbol{A}}{\partial t}\right)$$

$$\boldsymbol{E} = -\boldsymbol{\nabla}\phi - \frac{\partial \boldsymbol{A}}{\partial t}. \tag{2.18}$$

Then, we substitute equations 2.17 and 2.18 into equation 2.14 to obtain

$$\mu_0{}^{-1}\boldsymbol{\nabla}\times\boldsymbol{\nabla}\times\boldsymbol{A} = \varepsilon_0\frac{\partial}{\partial t}\left(-\boldsymbol{\nabla}\phi - \frac{\partial \boldsymbol{A}}{\partial t}\right) + \boldsymbol{J}$$

$$\boldsymbol{\nabla}(\boldsymbol{\nabla}\cdot\boldsymbol{A}) - \boldsymbol{\nabla}^2\boldsymbol{A} = \mu_0\varepsilon_0\left(-\frac{\partial \boldsymbol{\nabla}\phi}{\partial t} - \frac{\partial^2 \boldsymbol{A}}{\partial t^2}\right) + \mu_0\boldsymbol{J}$$

$$\nabla(\nabla\cdot\boldsymbol{A}) - \nabla^2\boldsymbol{A} + \frac{1}{c^2}\frac{\partial \boldsymbol{\nabla}\phi}{\partial t} + \frac{1}{c^2}\frac{\partial^2 \boldsymbol{A}}{\partial t^2} = \mu_0\boldsymbol{J}, \tag{2.19}$$

where the identity $\boldsymbol{\nabla}\times\boldsymbol{\nabla}\times\boldsymbol{A} = \boldsymbol{\nabla}(\boldsymbol{\nabla}\cdot\boldsymbol{A}) - \boldsymbol{\nabla}^2\boldsymbol{A}$ and relation $c = \frac{1}{\sqrt{\mu_0\varepsilon_0}}$ have been used. Similarly, we re-express equation 2.15 by substitute in equation 2.18 to obtain

$$\varepsilon_0 \boldsymbol{\nabla} \cdot \left(-\boldsymbol{\nabla}\phi - \frac{\partial \boldsymbol{A}}{\partial t} \right) = \rho$$

$$-\varepsilon_0 (\boldsymbol{\nabla} \cdot \boldsymbol{\nabla}\phi) - \varepsilon_0 \frac{\partial}{\partial t} (\boldsymbol{\nabla} \cdot \boldsymbol{A}) = \rho. \tag{2.20}$$

Then the Coulomb gauge which is specified by the condition $\boldsymbol{\nabla} \cdot \boldsymbol{A} = 0$ is imposed so that equations 2.19 and 2.20 can be further simplified into

$$-\boldsymbol{\nabla}^2 \boldsymbol{A} + \frac{1}{c^2} \frac{\partial \boldsymbol{\nabla}\phi}{\partial t} + \frac{1}{c^2} \frac{\partial^2 \boldsymbol{A}}{\partial t^2} = \mu_0 \boldsymbol{J} \tag{2.21}$$

and

$$-\boldsymbol{\nabla} \cdot \boldsymbol{\nabla}\phi = \frac{\rho}{\varepsilon_0}. \tag{2.22}$$

Notice that equation 2.22 shows that the scalar potential ϕ satisfies the Poisson's equation of electrostatics. Since the field quantisation is to be done on a free field (*i.e.* a radiation field that is free of current and charge), the variables $\boldsymbol{J}$ and ρ are set to zero. This simplifies equation 2.22 to Laplace equation which is in the form of

$$\boldsymbol{\nabla} \cdot \boldsymbol{\nabla}\phi = 0. \tag{2.23}$$

In this case, ϕ can be set to equal to zero so that equations 2.18 and 2.21 can be simplified as

$$\boldsymbol{E} = -\frac{\partial \boldsymbol{A}}{\partial t} \tag{2.24}$$

and

$$\boldsymbol{\nabla}^2 \boldsymbol{A} - \frac{1}{c^2} \frac{\partial^2 \boldsymbol{A}}{\partial t^2} = 0 \tag{2.25}$$

respectively. Note that equation 2.25 is actually a wave equation in terms of the vector potential $\boldsymbol{A}$.

Before moving onto the next section, it should be noted that other gauges such as Lorentz gauge can be equivalently used in the quantisation procedure. The choice of Coulomb gauge is justified by the fact that it is a transverse gauge which allows the electric field to be a transverse field. Since only transverse photons are present, the solution is practically simpler. On the contrary, Lorentz gauge contains both transverse and longitudinal components, hence it is not used in the derivations here for simplicity purpose.

2.3.2 Implications of the Wave Equation

Equation 2.25 from the previous section is a wave equation in terms of the vector potential $\boldsymbol{A}$ which can be expressed as

$$\boldsymbol{A} = \alpha q(t)\boldsymbol{u}(\boldsymbol{r}), \tag{2.26}$$

where α is a constant. We substitute equation 2.26 into equation 2.25 to give

$$\frac{\boldsymbol{\nabla}^2\boldsymbol{u}(\boldsymbol{r})}{\boldsymbol{u}(\boldsymbol{r})} = \frac{1}{c^2}\frac{\ddot{q}(t)}{q(t)}.$$

Since the position dependent terms and the time dependent terms are separated to the left and right sides of the equation respectively, both sides of the equation must be equal to a constant which is independent from the position and time variables. Let that constant be $-\boldsymbol{k}^2$, where $\boldsymbol{k}$ is a wave vector that depends on the boundary condition, we may then express the equation in the spatial form as

$$\boldsymbol{\nabla}^2\boldsymbol{u}(\boldsymbol{r}) + \boldsymbol{k}^2\boldsymbol{u}(\boldsymbol{r}) = 0$$

and in the temporal form as

$$\ddot{q}(t) + \boldsymbol{\omega}^2 q(t) = 0,$$

where $\boldsymbol{\omega} = c\boldsymbol{k}$.

Now we proceed to study the boundary conditions on the vector potential $\boldsymbol{A}$. Since it is assumed that the walls of the resonator are perfect conductors, the boundary conditions for dielectric-conductor boundary dictate that the tangential $\boldsymbol{E}$ field and the normal $\boldsymbol{B}$ field must vanish. Suppose that $\boldsymbol{e}_{\parallel}$ is a unit vector parallel to the boundary whereas $\boldsymbol{e}_{\perp}$is a unit vector perpendicular to the boundary, the parallel component of the $\boldsymbol{E}$ field at the boundary takes the form

$$\begin{aligned}\boldsymbol{e}_{\parallel}(\boldsymbol{r}) \cdot \boldsymbol{E}(\boldsymbol{r}, t) &= -\boldsymbol{e}_{\parallel}(\boldsymbol{r}) \cdot \frac{\partial \boldsymbol{A}}{\partial t} \\ &= -\alpha \dot{q}(t)[\boldsymbol{u}(\boldsymbol{r}) \cdot \boldsymbol{e}_{\parallel}(\boldsymbol{r})] \,.\end{aligned}$$

Since the tangential component of $\boldsymbol{E}$ field at the boundary must vanish, this leads to

$$\boldsymbol{u}(\boldsymbol{r}) \cdot \boldsymbol{e}_{\parallel}(\boldsymbol{r}) = 0 \,. \tag{2.27}$$

Similarly, the orthogonal component of the $\boldsymbol{B}$ field at the boundary takes the form

$$\begin{aligned}\boldsymbol{e}_{\perp}(\boldsymbol{r}) \cdot \boldsymbol{B}(\boldsymbol{r}, t) &= \boldsymbol{e}_{\perp}(\boldsymbol{r}) \cdot [\boldsymbol{\nabla} \times \boldsymbol{A}] \\ &= \alpha q(t)[\boldsymbol{e}_{\perp}(\boldsymbol{r}) \cdot (\boldsymbol{\nabla} \times \boldsymbol{u}(\boldsymbol{r}))] \,.\end{aligned}$$

Since the orthogonal component of the $\boldsymbol{B}$ field at the boundary must vanish, this leads to

$$\boldsymbol{e}_{\perp}(\boldsymbol{r}) \cdot \big(\boldsymbol{\nabla} \times \boldsymbol{u}(\boldsymbol{r})\big) = 0 \,. \tag{2.28}$$

It is important to note that the relations in equations 2.27 and 2.28 are only valid at the boundary. These two boundary conditions imply discrete property of the possible wave vectors. In other words, only a discrete set of mode functions $\boldsymbol{u}_k(\boldsymbol{r})$ is allowed in a resonator. The subscript k refers to a set of integer numbers. Such phenomenon is common for radiation field propagating inside a waveguide. In fact it is known that these mode functions obey orthonormality property given as

$$\int d^3r \, \boldsymbol{u}_k(\boldsymbol{r}) \cdot \boldsymbol{u}_{k'}(\boldsymbol{r}) = \delta_{k,k'} \,. \tag{2.29}$$

Note that the orthonormality of mode functions imposes a constraint such that $\int d^3r\,|\boldsymbol{u}_k|^2 = 1$. To satisfy this condition, the relation $\boldsymbol{u}_k = N\boldsymbol{v}_k$ is introduced, where N is the normalisation constant and $\boldsymbol{v}_k$ is a dimensionless mode function. The normalisation constant N is always in terms of the volume of the resonator, V and an algebraic factor. Therefore we introduce the effective mode volume V_k such that it contains both the volume of the resonator and the algebraic factor so that the normalisation constant is V_k. Hence the orthonormality condition in equation 2.29 becomes

$$\frac{1}{\sqrt{V_k V_{k'}}}\int d^3r\,\boldsymbol{u}_k(\boldsymbol{r})\cdot\boldsymbol{u}_{k'}(\boldsymbol{r}) = \delta_{k,k'}\,. \tag{2.30}$$

Furthermore it can be observed that the Coulomb gauge condition now takes the form of

$$\nabla\cdot\boldsymbol{u}_k(\boldsymbol{r}) = 0\,, \tag{2.31}$$

which is valid throughout the whole resonator.

2.3.3 Quantisation of the Radiation Field

In the previous section, it is shown that the boundary condition of the resonator causes the discreteness of the spatial part of the vector potential. However this has nothing to do with the quantisation of the radiation field, instead it is the time dependent part of the vector potential that is needed for the quantisation procedure. In this section, the quantisation of the radiation field in a resonator of arbitrary shape is formulated. We begin by first recalling the form of the vector potential in equation 2.26 and expand it into a discrete sum of mode functions which is in the form of

$$\boldsymbol{A} = \sum_k \frac{1}{\sqrt{\varepsilon_0 V_k}} q_k(t)\boldsymbol{v}_k(\boldsymbol{r}),$$

where ε_0 is the electric permittivity. Separate out the terms V_k and ε_0 for convenience and now the constant α is determined by these two factors. This

expression of the vector potential is then substituted into equations 2.17 and 2.18 so that we obtain

$$\boldsymbol{H}(\boldsymbol{r},t)=\frac{1}{\mu_0}\boldsymbol{\nabla}\times\boldsymbol{A}=\sum_k\frac{1}{\mu_0\sqrt{\varepsilon_0 V_k}}q_k(t)\big(\nabla\times\boldsymbol{v}_k(\boldsymbol{r})\big), \tag{2.32}$$

$$\boldsymbol{E}(\boldsymbol{r},t)=\frac{\partial\boldsymbol{A}}{\partial t}=\sum_k\frac{1}{\sqrt{\varepsilon_0 V_k}}\dot{q}_k(t)\boldsymbol{v}_k(\boldsymbol{r}). \tag{2.33}$$

Now we proceed to calculate the total energy of the electromagnetic field in the resonator. The Hamiltonian of the total field inside the resonator is dependent on the $\boldsymbol{E}$ field and $\boldsymbol{H}$ field and is expressed as

$$H=\int\left(\frac{1}{2}\varepsilon_0\boldsymbol{E}^2(\boldsymbol{r},t)+\frac{1}{2}\mu_0\boldsymbol{H}^2(\boldsymbol{r},t)\right)d^3r\,.$$

We substitute the aforementioned $\boldsymbol{E}$ field and $\boldsymbol{H}$ field into the Hamiltonian to gain the expression of

$$H=\frac{1}{2}\sum_k\sum_{k'}\frac{1}{\sqrt{V_kV_{k'}}}\dot{q}_k\dot{q_{k'}}\int\boldsymbol{v}_k\cdot\boldsymbol{v}_{k'}d^3r + \frac{c^2}{2}\sum_k\sum_{k'}\frac{1}{\sqrt{V_kV_{k'}}}q_kq_{k'}\int(\boldsymbol{\nabla}\times\boldsymbol{v}_k)\cdot(\boldsymbol{\nabla}\times\boldsymbol{v}_{k'})\,d^3r.$$

By making use of the identity $\boldsymbol{\nabla}\cdot(\boldsymbol{f}\times\boldsymbol{g})=\boldsymbol{g}\cdot(\boldsymbol{\nabla}\times\boldsymbol{f})-\boldsymbol{f}\cdot(\boldsymbol{\nabla}\times\boldsymbol{g})$ while letting $\boldsymbol{g}=\boldsymbol{\nabla}\times\boldsymbol{v}_k$ and $\boldsymbol{f}=\boldsymbol{v}_{k'}$, the identity becomes

$$\boldsymbol{\nabla}\cdot(\boldsymbol{v}_{k'}\times\boldsymbol{\nabla}\times\boldsymbol{v}_k)=(\boldsymbol{\nabla}\times\boldsymbol{v}_k)\cdot(\boldsymbol{\nabla}\times\boldsymbol{v}_{k'})-\boldsymbol{v}_{k'}\cdot(\boldsymbol{\nabla}\times\boldsymbol{\nabla}\times\boldsymbol{v}_k),$$

which can be rearranged into the form of

$$(\boldsymbol{\nabla}\times\boldsymbol{v}_k)\cdot(\boldsymbol{\nabla}\times\boldsymbol{v}_{k'})=\boldsymbol{\nabla}\cdot(\boldsymbol{v}_{k'}\times\boldsymbol{\nabla}\times\boldsymbol{v}_k)+\boldsymbol{v}_{k'}\cdot(\boldsymbol{\nabla}\times\boldsymbol{\nabla}\times\boldsymbol{v}_k).$$

We substitute this back into the Hamiltonian expression to obtain

$$H = \frac{1}{2}\sum_{k}\sum_{k'}\frac{1}{\sqrt{V_k V_{k'}}}\dot{q}_k \dot{q}_{k'}\int \boldsymbol{v}_k \cdot \boldsymbol{v}_{k'} d^3r + \frac{c^2}{2}\sum_{k}\sum_{k'}\frac{1}{\sqrt{V_k V_{k'}}} q_k q_{k'}\int \Big(\boldsymbol{\nabla}\cdot\big(\boldsymbol{v}_{k'}\times(\boldsymbol{\nabla}\times\boldsymbol{v}_k)\big) + \boldsymbol{v}_{k'} \cdot (\boldsymbol{\nabla}\times\boldsymbol{\nabla}\times\boldsymbol{v}_k)\Big)\, d^3r\,.$$

Using the Gauss theorem, the integral is converted into

$$\int \boldsymbol{\nabla}\cdot\big(\boldsymbol{v}_{k'}\times(\boldsymbol{\nabla}\times\boldsymbol{v}_k)\big)\, d^3r = \int \big(\boldsymbol{v}_{k'}\times(\boldsymbol{\nabla}\times\boldsymbol{v}_k)\big)\cdot d\boldsymbol{S}\,.$$

It is observed that $\boldsymbol{v}_{k'}$ is proportional to the spatial part of the electric field (equation 2.24) whereas $\boldsymbol{\nabla}\times\boldsymbol{v}_k$ is proportional to the spatial part of the magnetic field (equation 2.17). Since the electric field is orthogonal to the surface of the resonator and magnetic field is parallel to it, the cross product of these two vectors will always yield a vector that is perpendicular to the surface vector of the resonator; hence the surface integral vanishes. Moreover, another term may also be simplified as

$$\begin{aligned}\boldsymbol{\nabla}\times(\boldsymbol{\nabla}\times\boldsymbol{v}_k) &= \boldsymbol{\nabla}(\boldsymbol{\nabla}\cdot\boldsymbol{v}_k) - \boldsymbol{\nabla}^2\boldsymbol{v}_k \\ &= -\boldsymbol{\nabla}^2\boldsymbol{v}_k \\ &= \boldsymbol{k}_k^2\,\boldsymbol{v}_k \\ &= \left(\frac{\omega_k}{c}\right)^2 \boldsymbol{v}_k\,,\end{aligned}$$

where the Coulomb gauge condition in equation 2.31 and the identity $\boldsymbol{\nabla}\times(\boldsymbol{\nabla}\times\boldsymbol{f}) = \boldsymbol{\nabla}(\boldsymbol{\nabla}\cdot\boldsymbol{f}) - \boldsymbol{\nabla}^2\boldsymbol{f}$ are utilised. Finally, we make use of the orthonormality to obtain the final form of the Hamiltonian as

$$\begin{aligned}H &= \sum_k \left[\frac{1}{2}\dot{q}_k^2 + \frac{1}{2}\omega_k^2 q_k^2\right] \\ &= \sum_k H_k\,,\end{aligned} \tag{2.34}$$

where $H_k = \frac{1}{2}\dot{q}_k^2 + \frac{1}{2}\omega_k^2 q_k^2$. It is immediately recognised that the Hamiltonian of mode *k* (i.e. H_k) resembles the Hamiltonian of a harmonic oscillator. To confirm with this claim, the Hamilton equations of two conjugate variables q_k and $p_k = \dot{q}_k$ are $\dot{q}_k = \frac{\partial H_k}{\partial p_k} = p_k$ and $\dot{p}_k = -\frac{\partial H_k}{\partial q_k} = -\omega_k^2 q_k$, which lead to the equation of motion for harmonic oscillator

$$\ddot{q}_k + \omega_k^2 q_k = 0 \,.$$

This indicates that the electromagnetic field in a resonator consists of a discrete set of harmonic oscillators with energies H_k. Therefore we make use of the known quantum mechanical solution of a harmonic oscillator which has been covered in section 2.2, the Hamiltonian operator for each individual oscillator is

$$\hat{H}_k = \hbar\omega_k \left(\hat{a}_+ \hat{a}_- + \frac{1}{2}\right). \tag{2.35}$$

The Hamiltonian of the radiation field is then the sum of all these oscillators' Hamiltonian

$$\begin{aligned} \hat{H} &= \sum_k \left[\hbar\omega_k \hat{a}_+ \hat{a}_- + \frac{1}{2}\hbar\omega_k\right] \\ &= \sum_k [\hbar\omega_k \hat{a}_+ \hat{a}_-] + H_0 \,, \end{aligned} \tag{2.36}$$

where

$$\hat{H}_0 = \sum_k \left[\frac{1}{2}\hbar\omega_k\right]$$

is the vacuum energy. It is observed that the vacuum energy does not contain any operator in its expression; hence the Hamiltonian remains non-zero even when there is no radiation field present. Moreover the frequencies ω_k have no upper bound and thus the vacuum energy term is infinite.

2.4 Three Pictures of Quantum Mechanics

2.4.1 Schrodinger Picture

In Schrodinger picture, quantum system is described by time dependent wavefunction which satisfies the Schrodinger equation,

$$\frac{d}{dt}|\Psi_S(t)\rangle = -\frac{i}{\hbar}\hat{H}_S|\Psi_S(t)\rangle, \tag{2.37}$$

where $|\Psi_S(t)\rangle$ and $\hat{H}_S$ are the wavefunction and Hamiltonian of the quantum system respectively in Schrodinger picture. The time factors can in fact be factored out as a separable solution, so that

$$|\Psi_S(t)\rangle = \exp\left(\frac{-i\hat{H}_S t}{\hbar}\right)|\Psi_S 0\rangle. \tag{2.38}$$

In contrast, the observables are represented by Hermitian operators which act on the wavefunction. These operators are time independent in Schrodinger picture.

2.4.2 Heisenberg Picture

Heisenberg picture has opposite traits compared to Schrodinger picture. In this picture, the operator is time dependent whereas the wavefunction is time independent. Transformation from Schrodinger picture to Heisenberg picture can be achieved using unitary transformation to eliminate the time dependence factor in the wavefunction in Schrodinger picture, such that

$$\begin{aligned}|\Psi_H\rangle &= \hat{U}|\Psi_S(t)\rangle \\ &= \exp\left(\frac{i\hat{H}_S t}{\hbar}\right)|\Psi_S(t)\rangle \\ &= |\Psi_S(0)\rangle,\end{aligned}$$

where $\hat{U} = \exp\left(\frac{i\hat{H}_S t}{\hbar}\right)$ and Ψ_H is the wavefunction in Heisenberg picture which is time independent. By taking the inner product of Ψ_H, we observe that

$$\langle \Psi_H | \Psi_H \rangle = \left\langle \exp\left(\frac{-i\hat{H}_S t}{\hbar}\right) \Psi_S(t) \middle| \exp\left(\frac{i\hat{H}_S t}{\hbar}\right) \Psi_S(t) \right\rangle$$
$$= \langle \Psi_S(t) | \Psi_S(t) \rangle.$$

To include the time dependence factor into the operator, we take the expectation value of the observable to be

$$\langle \hat{O} \rangle = \langle \Psi_S(t) | \hat{O}_S | \Psi_S(t) \rangle$$
$$= \left\langle \Psi_S(0) \left| \exp\left(\frac{i\hat{H}_S t}{\hbar}\right) \hat{O}_S \exp\left(\frac{-i\hat{H}_S t}{\hbar}\right) \right| \Psi_S(0) \right\rangle$$
$$= \langle \Psi_S(0) | \hat{O}_H | \Psi_S(0) \rangle$$
$$= \langle \Psi_H | \hat{O}_H | \Psi_H \rangle.$$

Therefore the observable operator in Heisenberg picture picks up the time dependence factor through unitary transformation, where

$$\hat{O}_H(t) = \exp\left(\frac{i\hat{H}_S t}{\hbar}\right) \hat{O}_S \exp\left(\frac{-i\hat{H}_S t}{\hbar}\right).$$

Heisenberg equation may be obtained by differentiating this operator as follows,

$$\frac{d\hat{O}_H}{dt} = \frac{i}{\hbar} \hat{H}_S \hat{O}_H + \exp\left(\frac{i\hat{H}_S t}{\hbar}\right) \frac{d\hat{O}_S}{dt} \exp\left(\frac{-i\hat{H}_S t}{\hbar}\right) - \frac{i}{\hbar} \hat{O}_H \hat{H}_S$$
$$= \frac{i}{\hbar} [\hat{H}_S, \hat{O}_H] + \exp\left(\frac{i\hat{H}_S t}{\hbar}\right) \frac{d\hat{O}_S}{dt} \exp\left(\frac{-i\hat{H}_S t}{\hbar}\right). \quad (2.39)$$

2.4.3 Interaction Picture

Interaction picture, also known as Dirac picture allows both the wavefunction and the operator to carry the time dependence traits. It is an intermediary between Schrodinger picture and Heisenberg picture which can be very useful in solving problems involving time-dependent interaction Hamiltonian.

Firstly the free term and the interaction term in the Hamiltonian in the Schrodinger picture are separated, so that

$$\hat{H}_S = \hat{H}_{S,0} + \hat{H}_{S,int}, \tag{2.40}$$

where $\hat{H}_{S,o}$ and $\hat{H}_{S,int}$ are the free unperturbed term and the small interaction perturbation term respectively in Schrodinger picture. From the experience in transforming Heisenberg picture, the wavefunction and the operator in interaction picture can be transformed in a similar manner using unitary transformation, such that

$$|\Psi_I(t)\rangle = \hat{U}|\Psi_S(t)\rangle = \exp\left(\frac{i\hat{H}_{S,O}t}{\hbar}\right)|\Psi_S(t)\rangle, \tag{2.41}$$

$$\hat{O}_I(t) = \exp\left(\frac{i\hat{H}_{S,O}t}{\hbar}\right)\hat{O}_S \exp\left(\frac{-i\hat{H}_{S,O}t}{\hbar}\right), \tag{2.42}$$

where $\Psi_I(t)$ and $\hat{O}_I(t)$ are the wavefunction and observable operator respectively in Heisenberg picture. We differentiate equation 2.41 with respect to time to yield

$$\begin{aligned}\frac{d}{dt}|\Psi_I(t)\rangle &= \frac{i}{\hbar}\hat{H}_{S,0}\ \exp\left(\frac{i\hat{H}_{S,O}t}{\hbar}\right)|\Psi_S(t)\rangle + \exp\left(\frac{i\hat{H}_{S,O}t}{\hbar}\right)\frac{d}{dt}|\Psi_S(t)\rangle \\ &= \frac{i}{\hbar}\hat{H}_{S,0}\,|\Psi_I(t)\rangle + \exp\left(\frac{i\hat{H}_{S,O}t}{\hbar}\right)\left(-\frac{i}{\hbar}\hat{H}_S|\Psi_S(t)\rangle\right) \\ &= \frac{i}{\hbar}\hat{H}_{S,0}\,|\Psi_I(t)\rangle - \frac{i}{\hbar}\left(\hat{H}_{S,0} + \hat{H}_{S,int}\right)|\Psi_I(t)\rangle \\ &= -\frac{i}{\hbar}\hat{H}_{S,int}|\Psi_I(t)\rangle. \end{aligned} \tag{2.43}$$

This form indicates that the state vector in interaction picture evolves in time according to the interaction term only. Next, equation 2.42 can also be differentiated with respect to time to obtain

$$\begin{aligned}\frac{d}{dt}\hat{O}_I(t) &= \frac{i}{\hbar}\hat{H}_{S,0}\hat{O}_I + \exp\left(\frac{i\hat{H}_{S,O}t}{\hbar}\right)\frac{d\hat{O}_S}{dt}\exp\left(\frac{-i\hat{H}_{S,O}t}{\hbar}\right) - \frac{i}{\hbar}\hat{O}_I\hat{H}_{S,0} \\ &= \frac{i}{\hbar}\left[\hat{H}_{S,0}, \hat{O}_I\right] + \exp\left(\frac{i\hat{H}_{S,O}t}{\hbar}\right)\frac{d\hat{O}_S}{dt}\exp\left(\frac{-i\hat{H}_{S,O}t}{\hbar}\right). \end{aligned} \tag{2.44}$$

Barnett and Radmore (1997) showed that the transformation of the Hamiltonian from Schrodinger picture to interaction picture can be obtained by solving the Schrodinger equation in interaction picture, such that

$$\begin{aligned}\widehat{H}_I|\Psi_I(t)\rangle &= i\hbar\frac{\partial}{\partial t}|\Psi_I(t)\rangle \\ \widehat{H}_I\widehat{U}|\Psi_S(t)\rangle &= i\hbar\frac{\partial}{\partial t}\left(\widehat{U}|\Psi_S(t)\rangle\right) \\ &= i\hbar\frac{\partial\widehat{U}}{\partial t}|\Psi_S(t)\rangle + i\hbar\widehat{U}\frac{\partial}{\partial t}|\Psi_S(t)\rangle \\ &= i\hbar\frac{\partial\widehat{U}}{\partial t}|\Psi_S(t)\rangle + \widehat{U}\widehat{H}_S|\Psi_S(t)\rangle.\end{aligned}$$

Hence by comparison, the transformation is obtained to be

$$\widehat{H}_I = i\hbar\frac{\partial\widehat{U}}{\partial t}\widehat{U}^\dagger + \widehat{U}\widehat{H}_S\widehat{U}^\dagger. \tag{2.45}$$

2.5 Exponential of Diagonal Matrices

The exponential of a two-by-two diagonal matrix is shown to take the form of

$$e^A = \begin{pmatrix} e^{c_{11}} & 0 \\ 0 & e^{c_{22}} \end{pmatrix},$$

where A is a diagonal matrix which is represented as

$$A = \begin{pmatrix} c_{11} & 0 \\ 0 & c_{22} \end{pmatrix}.$$

The mathematical proof of this formula is shown in this section. We first take the Taylor series of an exponential which is known as

$$e^x = 1 + x + \frac{x^2}{2!} + \frac{x^3}{3!} + \cdots,$$

and let A be a two by two matrix represented as

$$A = \begin{pmatrix} c_{11} & c_{12} \\ c_{21} & c_{22} \end{pmatrix},$$

so that the exponential of matrix A is simply

$$e^{A} = I + A + \frac{A^2}{2!} + \frac{A^3}{3!} + \cdots.$$

For a general form of matrix A, there is no simple solution to compute the power of the matrix. However, the solution is greatly simplified for diagonal matrix where the coefficients c_{12} and c_{21} are equal to zero so that

$$A = \begin{pmatrix} c_{11} & 0 \\ 0 & c_{22} \end{pmatrix},$$

then an arbitrary power n of the matrix is simply

$$A^n = \begin{pmatrix} c_{11}^n & 0 \\ 0 & c_{22}^n \end{pmatrix}.$$

Hence the exponential of the diagonal matrix may be significantly simplified and takes the form of

$$\begin{aligned} e^{A} &= \begin{pmatrix} 1 & 0 \\ 0 & 1 \end{pmatrix} + \begin{pmatrix} c_{11} & 0 \\ 0 & c_{22} \end{pmatrix} + \frac{1}{2!}\begin{pmatrix} c_{11}^2 & 0 \\ 0 & c_{22}^2 \end{pmatrix} + \cdots \\ &= \begin{pmatrix} 1 + c_{11} + \frac{1}{2!}c_{11}^2 + \cdots & 0 \\ 0 & 1 + c_{22} + \frac{1}{2!}c_{22}^2 + \cdots \end{pmatrix} \\ &= \begin{pmatrix} e^{c_{11}} & 0 \\ 0 & e^{c_{22}} \end{pmatrix}. \end{aligned} \tag{2.46}$$

2.6 Coherent State

Coherent state is a special class of field states that is an accurate representation of field produced by a stabilised laser. Its state $|\alpha\rangle$ can be expressed as a linear superposition of number states $|n\rangle$ which is in the form of

$$|\alpha\rangle = \exp\left(-\frac{1}{2}|\alpha|^2\right)\sum_{n=0}^{\infty}\frac{\alpha^n}{(n!)^{\frac{1}{2}}}\,|n\rangle, \tag{2.47}$$

where α is a complex number. It can be easily shown that $|\alpha\rangle$ is normalised by taking its inner product, such that

$$\begin{aligned}\langle\alpha|\alpha\rangle &= \exp(-|\alpha|^2)\sum_{n=0}^{\infty}\frac{{\alpha^*}^n\alpha^n}{n!}\\ &= \exp(-|\alpha|^2)\sum_{n=0}^{\infty}\frac{|\alpha|^{2n}}{n!}\\ &= \exp(-|\alpha|^2)\exp(|\alpha|^2)\\ &= 1.\end{aligned}$$

One key feature of coherent state is that $|\alpha\rangle$ is the right eigenstate of $\hat{a}_-$ operator with eigenvalue α. This can be easily shown as follows,

$$\begin{aligned}\hat{a}_-|\alpha\rangle &= \exp\left(-\frac{1}{2}|\alpha|^2\right)\sum_{n=1}^{\infty}\frac{\alpha^n}{(n!)^{\frac{1}{2}}}\sqrt{n}|n-1\rangle\\ &= \exp\left(-\frac{1}{2}|\alpha|^2\right)\sum_{n=1}^{\infty}\frac{\alpha^n}{\sqrt{(n-1)!}}\,|n-1\rangle\\ &= \exp\left(-\frac{1}{2}|\alpha|^2\right)\sum_{m=0}^{\infty}\frac{\alpha^{m+1}}{\sqrt{m!}}\,|m\rangle\\ &= \exp\left(-\frac{1}{2}|\alpha|^2\right)\sum_{m=0}^{\infty}\frac{\alpha^m\alpha}{\sqrt{m!}}\,|m\rangle\\ &= \alpha|\alpha\rangle.\end{aligned} \tag{2.48}$$

On the other hand, since the operators $\hat{a}_+$ and $\hat{a}_-$ do not commute, $|\alpha\rangle$ is naturally not the right eigenstate of $\hat{a}_+$. Instead, $|\alpha\rangle$ is the left eigenstate of $\hat{a}_+$ with eigenvalue α^*, i.e.

$$\begin{aligned}
\langle\alpha|\hat{a}_+ &= \hat{a}_-\langle\alpha| \\
&= \exp\left(-\frac{1}{2}|\alpha|^2\right)\sum_{n=1}^{\infty}\frac{{\alpha^*}^n}{(n!)^{\frac{1}{2}}}\sqrt{n-1}\langle n-1| \\
&= \exp\left(-\frac{1}{2}|\alpha|^2\right)\sum_{n=1}^{\infty}\frac{{\alpha^*}^n}{\sqrt{(n-1)!}}\langle n-1| \\
&= \exp\left(-\frac{1}{2}|\alpha|^2\right)\sum_{m=1}^{\infty}\frac{{\alpha^*}^{m+1}}{\sqrt{m!}}\langle m| \\
&= \exp\left(-\frac{1}{2}|\alpha|^2\right)\sum_{m=1}^{\infty}\frac{{\alpha^*}^m\alpha^*}{\sqrt{m!}}\langle m| \\
&= \alpha^*\langle\alpha|. \qquad (2.49)
\end{aligned}$$

By making use of the results from equations 2.47, 2.48 and 2.49, we derive the mean photon number in coherent state as follows,

$$\begin{aligned}
\bar{n} &= \langle\alpha|\hat{n}|\alpha\rangle \\
&= \langle\alpha|\hat{a}_+\hat{a}_-|\alpha\rangle \\
&= \langle\alpha|\alpha^*\alpha|\alpha\rangle \\
&= |\alpha|^2. \qquad (2.50)
\end{aligned}$$

Hence the photon number probability distribution for coherent state can be expressed as

$$\begin{aligned}
P(n) &= |\langle n|\alpha\rangle|^2 \\
&= \frac{\exp(-|\alpha|^2)\,|\alpha|^{2n}}{n!} \\
&= \frac{[\exp(-\bar{n})\;\bar{n}^n]}{n!}. \qquad (2.51)
\end{aligned}$$

2.7 Thermal State

When insufficient amount of information is known, the field state can be expressed as a mixed state represented by a density matrix. Thermal state is a kind of mixed state that is utilised when minimum amount of information is given, knowing only the mean value of energy. The density matrix of a thermal state is expressed as

$$\hat{\rho} = \sum_{n=0}^{\infty} P(n)\ |n\rangle\langle n|, \tag{2.52}$$

where $P(n) = \left\{1 - \exp\left(-\frac{\hbar\omega}{k_B T}\right)\right\} \exp\left(-\frac{n\hbar\omega}{k_B T}\right)$ is the probability of state $|n\rangle$ being measured. To derive for the expression of the mean photon number, the expression for $P(n)$ is first simplified into

$$\begin{aligned} P(n) &= \langle n|\hat{\rho}|n\rangle \\ &= Tr(\hat{\rho}|n\rangle\langle n|), \end{aligned}$$

where the identity $\langle a|b\rangle = Tr(|b\rangle\langle a|)$ is used. Then the mean photon number is simply

$$\begin{aligned} \bar{n} &= \sum_{n=0}^{\infty} nP(n) \\ &= \sum_{n=0}^{\infty} n\ Tr(\hat{\rho}|n\rangle\langle n|) \\ &= \sum_{n=0}^{\infty} n\ Tr\left(\left\{\sum_{n=0}^{\infty} P(n)\ |n\rangle\langle n|\right\}|n\rangle\langle n|\right) \\ &= Tr\left(\sum_{n=0}^{\infty} P(n)\ n|n\rangle\langle n|\right). \end{aligned}$$

We make use of the relation $\hat{n}|n\rangle = n|n\rangle$, so that the expression of mean photon number may be simplified into

$$\bar{n} = Tr\left(\sum_{n=0}^{\infty} P(n)\,\hat{n}|n\rangle\langle n|\right)$$
$$= Tr(\hat{\rho}\hat{n}). \tag{2.53}$$

Substitute equation 2.52 into equation 2.53, we therefore obtain

$$\bar{n} = \left\{1 - \exp\left(-\frac{\hbar\omega}{k_B T}\right)\right\}\sum_{n=0}^{\infty} n\left[\exp\left(-\frac{n\hbar\omega}{k_B T}\right)\right].$$

We let $x = \exp\left(-\frac{\hbar\omega}{k_B T}\right)$, the mean photon number can then be rewritten as

$$\bar{n} = \{1 - x\}\sum_{n=0}^{\infty} nx^n$$
$$= \{1 - x\}\sum_{n=0}^{\infty} x\frac{d}{dx}(x^n)$$
$$= \{1 - x\}\{x\}\frac{d}{dx}\sum_{n=0}^{\infty} x^n$$
$$= \{1 - x\}\{x\}\frac{d}{dx}\left(\frac{1}{1-x}\right)$$
$$= \{1 - x\}\{x\}(1-x)^{-2}$$
$$= \frac{x}{1-x}$$
$$= \frac{1}{x^{-1} - 1}$$
$$= \frac{1}{\exp\left(\frac{\hbar\omega}{k_B T}\right) - 1}.$$

We rearrange the expression so that

$$\exp\left(\frac{\hbar\omega}{k_B T}\right) = \frac{1}{\bar{n}} + 1$$
$$= \frac{1 + \bar{n}}{\bar{n}},$$

which can then be inverted so that

$$\exp\left(-\frac{\hbar\omega}{k_B T}\right) = \frac{\bar{n}}{1+\bar{n}}. \tag{2.54}$$

Substitute equation 2.54 back into the original probability function $P(n)$, we therefore obtain

$$\begin{aligned} P(n) &= \left\{1 - \frac{\bar{n}}{1+\bar{n}}\right\}\frac{\bar{n}}{1+\bar{n}} \\ &= \left\{\frac{1}{1+\bar{n}}\right\}\frac{\bar{n}}{1+\bar{n}} \\ &= \frac{\bar{n}}{(1+\bar{n})^2}. \end{aligned} \tag{2.55}$$

CHAPTER 3

METHODOLOGY AND WORK PLAN

3.1 Derivations in Semiclassical Treatment

Firstly, the total Hamiltonian of a quantum mechanical two-level system being coupled to a monochromatic classical radiation field with frequency ω was formulated. The expression of the electric field intensity $\boldsymbol{E}$ was obtained by assuming dipole approximation to eliminate the spatial dependence factor of the field. Then the atomic Hamiltonian of the two-level system is formulated by assuming the ground state's energy as zero. Next, the interaction Hamiltonian which is predominantly contributed by electric-dipole Hamiltonian was formulated. For this part, several methods such as minimal coupling and direct coupling could have been used, however direct coupling was utilised because of its conceptual simplicity. By using several identities, the expression of the dipole operator was derived. The interaction Hamiltonian is finally simplified using rotating-wave approximation to eliminate fast rotation factors.

The total Hamiltonian was obtained by summing the atomic Hamiltonian and the interaction Hamiltonian, which was then substituted into the Schrodinger equation. The resulting differential equations were solved to obtain the expressions of the coefficients of the wavefunction. With the available expressions and assumption of initially unexcited atom, the solution of resonant case $\Delta = 0$ was obtained. The graph depicting probability of atom in each state against Ωt was plotted using MATLAB software, where Ω is the Rabi frequency and t is the time. Finally similar procedures were repeated for near resonant case.

3.2 Derivations in Quantum Mechanical Treatment

The full quantum mechanical treatment on light-matter interaction assumed single-mode quantised light field of various initial field statistics interacting with an energetically quantised two-level atom. The objective of this treatment is to derive the field-atom wavefunction of the joint interaction system using Jaynes-Cummings Model.

Firstly, the quantisation of electromagnetic field which was assumed to be a free field contained inside a closed resonator with perfectly conducting walls was derived and reported. Various properties of quantum field states such as number states, coherent states and thermal states were reported. The understanding on these quantum fields serves as the foundation to apply different types of initial light sources in the interaction. The transformations between Hamiltonians in different pictures (i. e. Schrodinger picture, Heisenberg picture and Interaction picture) were also investigated and reported.

With all the available resources, the interaction system may then be derived using Jaynes-Cummings model. The atomic Hamiltonian, field Hamiltonian and interaction Hamiltonian, all in Schrodinger picture, were derived and combined to form the total Hamiltonian of the system. Then the total Hamiltonian in Schrodinger picture was transformed into interaction picture using the transformation relation derived previously. The rotating-wave approximation was applied to the resulting total Hamiltonian which was then used to solve the Schrodinger equation. Using similar manner as in semiclassical treatment, the coefficients of the wavefunction were derived using algebraic operations.

After solving for the coefficients c_1 and c_2, the modulus square of c_1 was calculated to plot for the graph of ground state probability against time using MATLAB software. The probability here refers to the probability of the two-level atom to stay in ground state at any time t. However it is found that the coefficients depend on the initial field statistics, therefore the probability function of the initial field state had to be included in the derived equation to yield numerical solutions. In this study, number state, coherent state and thermal state were used to study the characteristics of light-matter interaction in quantum mechanical treatment. Both the cases of resonant and near resonant were applied here. The relationship between the probability functions and the parameters such as interaction strength, mean photon number and detuning were studied and discussed extensively.

CHAPTER 4

RESULTS AND DISCUSSIONS

4.1 Semiclassical Treatment

4.1.1 Classical Electromagnetic Field

We consider the simplest case of coupling a classical field to a quantum mechanical two-level atom. It is assumed that the classical field is monochromatic with frequency ω. Dipole approximation is also utilised so that the spatial dependence factor of the field equals to unity. This is fully justifiable as long as the wavelength λ is significantly greater than the dimension of the atom so that $kr \ll 1$, which leads to $e^{ikr} \approx 1$. The electric field of light may then be written as follows,

$$\begin{aligned} \boldsymbol{E}(t) &= \boldsymbol{\varepsilon} E_0 \cos \omega t \\ &= \boldsymbol{\varepsilon} E_0 \frac{1}{2}\left(e^{-i\omega t} + e^{i\omega t}\right) \\ &= \boldsymbol{\varepsilon} E_0 \frac{1}{2} e^{-i\omega t} + \boldsymbol{\varepsilon} E_0 \frac{1}{2}\, e^{i\omega t} \\ &= \boldsymbol{E}^{+}(t) + \boldsymbol{E}^{-}(t), \end{aligned} \tag{4.1}$$

where $\boldsymbol{\varepsilon}$ is the unit polarisation of the vector field, $\boldsymbol{E}^{+}(t) = \boldsymbol{\varepsilon} E_0 \frac{1}{2} e^{-i\omega t}$ and $\boldsymbol{E}^{-}(t) = \boldsymbol{\varepsilon} E_0 \frac{1}{2}\, e^{i\omega t}$.

4.1.2 Atomic Hamiltonian

Next, we proceed to derive the Hamiltonian of a two-level atom which is assumed to have state 1 (ground state) with frequency ω_1 and state 2 (excited state) with frequency ω_2. Hence the atomic Hamiltonian can be expressed as

$$\widehat{H}_A = \hbar\omega_2 |2\rangle\langle 2| + \hbar\omega_1 |1\rangle\langle 1|.$$

In general, the relative energy difference between the two levels is more important rather than the absolute energy values, thus the Hamiltonian may be simplified by assuming $\omega_1 = 0$, then

$$\hat{H}_A = \hbar\omega_2|2\rangle\langle 2|. \tag{4.2}$$

Before moving on, it is now important to clarify that the detuning $\Delta = \omega - \omega_2$ is sufficiently small so that the two-level atom model stays valid. Otherwise at high detuning, the energy of the classical field may be sufficient to excite the electron to a third level.

4.1.3 Interaction Hamiltonian

The Hamiltonian of interaction between the light field and the atom is formulated in this section. The interaction Hamiltonian is predominantly contributed by the electric-dipole interaction (Loudon, 2000). Suppose there are *Z* numbers of electrons in the two-level atom, the classical result from the literature shows that the Hamiltonian takes the form

$$\hat{H}_I = -\hat{\boldsymbol{d}} \cdot \boldsymbol{E}, \tag{4.3}$$

where $\hat{\boldsymbol{d}} = -e\sum_{i=1}^{Z} \boldsymbol{r_i}$ is the dipole operator, *e* is the elementary charge and $\boldsymbol{r_i}$ is the position vector of each electron *i*.

Since the interaction Hamiltonian is real and has odd parity, it is immediately concluded that $\langle 1|\hat{\boldsymbol{d}}|1\rangle = \langle 2|\hat{\boldsymbol{d}}|2\rangle = 0$ and $\langle 1|\hat{\boldsymbol{d}}|2\rangle = \langle 2|\hat{\boldsymbol{d}}|1\rangle^* \neq 0$ provided that the two atomic states have opposite parity. While the aforementioned equation is a complex quantity in general, it is real for transitions between bound states (Loudon, 2000). Therefore, the expressions can then be equated to each other as

$$\langle 1|\hat{\boldsymbol{d}}|2\rangle = \langle 2|\hat{\boldsymbol{d}}|1\rangle. \tag{4.4}$$

Following that, the identity $(|2\rangle\langle 2| + |1\rangle\langle 1|)$ is used to express the dipole operator $\hat{\boldsymbol{d}}$ into the following form,

$$\begin{aligned}\hat{\boldsymbol{d}} &= (|2\rangle\langle 2| + |1\rangle\langle 1|)\,\hat{\boldsymbol{d}}\,(|2\rangle\langle 2| + |1\rangle\langle 1|)\\ &= |2\rangle\langle 2|\hat{\boldsymbol{d}}|2\rangle\langle 2| + |2\rangle\langle 2|\hat{\boldsymbol{d}}|1\rangle\langle 1| + |1\rangle\langle 1|\hat{\boldsymbol{d}}|2\rangle\langle 2| + |1\rangle\langle 1|\hat{\boldsymbol{d}}|1\rangle\langle 1|\\ &= |2\rangle\langle 2|\hat{\boldsymbol{d}}|1\rangle\langle 1| + |1\rangle\langle 1|\hat{\boldsymbol{d}}|2\rangle\langle 2|.\end{aligned}$$

Let $\hat{\sigma}^- = |1\rangle\langle 2|$ and $\hat{\sigma}^+ = |2\rangle\langle 1|$, while applying the relationship in equation 4.4, then it is obtained $\hat{\boldsymbol{d}} = \langle 1|\hat{\boldsymbol{d}}|2\rangle\sigma^- + \langle 1|\hat{\boldsymbol{d}}|2\rangle\sigma^+$.

It is worth discussing on the physical significance of $\hat{\sigma}^-$ and $\hat{\sigma}^+$ operators. If these operators are applied on an arbitrary state $|\psi\rangle = c_1|1\rangle + c_2|2\rangle$, the results yield $\sigma^+|\psi\rangle = c_1|2\rangle$ and $\sigma^-|\psi\rangle = c_2|1\rangle$. This means that $\hat{\sigma}^+$ causes a transition from state 1 to state 2, whereas $\hat{\sigma}^-$ causes a transition from state 2 to state 1. In fact, if the expectation value of $\hat{\sigma}^-$ is computed, we obtain

$$\begin{aligned}\langle\hat{\sigma}^-\rangle &= (c_1{}^*\langle 1| + c_2{}^*\langle 2|)\,\hat{\sigma}^-\,(c_1|1\rangle + c_2|2\rangle)\\ &= (c_1{}^*\langle 1| + c_2{}^*\langle 2|)\,(|1\rangle\langle 2|)\,(c_1|1\rangle + c_2|2\rangle)\\ &= c_1{}^* c_2\,.\end{aligned}$$

Similarly the expectation value of the operator $\hat{\sigma}^+$ is $\langle\hat{\sigma}^+\rangle = c_2{}^* c_1$.

Since the Hamiltonian is now explicitly depending on time, we let the time factor be absorbed by the coefficients so that $c_1 \sim e^{-i\omega_1 t}$ and $c_2 \sim e^{-i\omega_2 t}$. Therefore it is obvious that $\hat{\sigma}^- \sim e^{-i(\omega_2-\omega_1)t}$ and $\hat{\sigma}^+ \sim e^{i(\omega_2-\omega_1)t}$. Hence the dipole operator may be simplified into

$$\hat{\boldsymbol{d}} = \hat{\boldsymbol{d}}^+ + \hat{\boldsymbol{d}}^-,$$

where $\hat{\boldsymbol{d}}^+ = \langle 1|\hat{\boldsymbol{d}}|2\rangle\hat{\sigma}^-$ and $\hat{\boldsymbol{d}}^- = \langle 1|\hat{\boldsymbol{d}}|2\rangle\hat{\sigma}^+$. Rewriting the interaction Hamiltonian in equation 4.3, we therefore obtain

$$\begin{aligned}\hat{H}_I &= -\left(\left(\hat{\boldsymbol{d}}^+ + \hat{\boldsymbol{d}}^-\right)\cdot(\boldsymbol{E}^+ + \boldsymbol{E}^-)\right)\\ &= -\left(\hat{\boldsymbol{d}}^+\cdot\boldsymbol{E}^+ + \hat{\boldsymbol{d}}^+\cdot\boldsymbol{E}^- + \hat{\boldsymbol{d}}^-\cdot\boldsymbol{E}^+ + \hat{\boldsymbol{d}}^-\cdot\boldsymbol{E}^-\right).\end{aligned}$$

Since $|\omega - \omega_2| \ll \omega + \omega_2$, this means that $\hat{\boldsymbol{d}}^+\cdot\boldsymbol{E}^+$ and $\hat{\boldsymbol{d}}^-\cdot\boldsymbol{E}^-$ rotate rapidly and can therefore be approximated as zero average value (Steck, 2007). Such

approximation is known as rotating-wave approximation. Thus the interaction Hamiltonian becomes

$$\begin{aligned}\hat{H}_I &= -\left(\hat{\boldsymbol{d}}^+ \cdot \boldsymbol{E}^- + \hat{\boldsymbol{d}}^- \cdot \boldsymbol{E}^+\right) \\ &= -\langle 1|\hat{\boldsymbol{d}}|2\rangle \cdot \boldsymbol{\varepsilon} E_0 \frac{1}{2}\left(\hat{\sigma}^- e^{i\omega t} + \hat{\sigma}^+ e^{-i\omega t}\right).\end{aligned}$$

We now define the Rabi frequency as

$$\Omega = \frac{-\langle 1|\hat{\boldsymbol{d}}|2\rangle \cdot \boldsymbol{\varepsilon} E_0}{\hbar}$$

which therefore simplifies the interaction Hamiltonian as

$$\hat{H}_I = \frac{\hbar\Omega}{2}\left(\hat{\sigma}^- e^{i\omega t} + \hat{\sigma}^+ e^{-i\omega t}\right). \tag{4.5}$$

4.1.4 Total Hamiltonian and Schrödinger equation

The total Hamiltonian may be obtained by summing the atomic Hamiltonian in equation 4.2 and the interaction Hamiltonian from equation 4.5, so that

$$\begin{aligned}\hat{H} &= \hat{H}_A + \hat{H}_I \\ &= \hbar\omega_2|2\rangle\langle 2| + \frac{\hbar\Omega}{2}\left(\hat{\sigma}^- e^{i\omega t} + \hat{\sigma}^+ e^{-i\omega t}\right) \\ &= \hbar\omega_2|2\rangle\langle 2| + \frac{\hbar\Omega}{2}\left(e^{i\omega t}\,|1\rangle\langle 2| + e^{-i\omega t}\,|2\rangle\langle 1|\right).\end{aligned}$$

Suppose the two-level atom is represented by a wavefunction $|\psi\rangle = c_1|1\rangle + c_2|2\rangle$, then it is possible to solve the Schrödinger equation to give

$$\begin{aligned}i\hbar\frac{dc_1}{dt}|1\rangle + i\hbar\frac{dc_2}{dt}|2\rangle &= \hbar\omega_2 c_2|2\rangle + \frac{\hbar\Omega}{2}e^{i\omega t}c_2\,|1\rangle + \frac{\hbar\Omega}{2}e^{-i\omega t}c_1\,|2\rangle \\ \frac{dc_1}{dt}|1\rangle + \frac{dc_2}{dt}|2\rangle &= -i\omega_2 c_2|2\rangle - \frac{i\Omega}{2}e^{i\omega t}c_2\,|1\rangle - \frac{i\Omega}{2}e^{-i\omega t}c_1\,|2\rangle.\end{aligned}$$

The forms of $|1\rangle$ and $|2\rangle$ for both sides of the equation are compared and we obtain

$$\frac{dc_1}{dt} = -\frac{i\Omega}{2} e^{i\omega t} c_2, \tag{4.6}$$

and

$$\frac{dc_2}{dt} = -i\omega_2 c_2 - \frac{i\Omega}{2} e^{-i\omega t} c_1. \tag{4.7}$$

To further simplify equation 4.7, we let $\widetilde{c_2} = e^{i\omega t} c_2$ to eliminate fast rotation so that its time derivative is

$$\frac{d\widetilde{c_2}}{dt} = i\omega e^{i\omega t} c_2 + e^{i\omega t} \frac{dc_2}{dt},$$

which can be rearranged into the form of

$$\frac{dc_2}{dt} = e^{-i\omega t} \frac{d\widetilde{c_2}}{dt} - i\omega e^{-i\omega t} \widetilde{c_2}\,.$$

We substitute this expression into equation 4.7 to obtain

$$\begin{aligned} e^{-i\omega t} \frac{d\widetilde{c_2}}{dt} - i\omega e^{-i\omega t} \widetilde{c_2} &= -i\omega_2 c_2 - \frac{i\Omega}{2} e^{-i\omega t} c_1 \\ \frac{d\widetilde{c_2}}{dt} &= -i\omega_2 c_2 e^{i\omega t} + i\omega \widetilde{c_2} - \frac{i\Omega}{2} c_1 \\ \frac{d\widetilde{c_2}}{dt} &= i\Delta \widetilde{c_2} - \frac{i\Omega}{2} c_1, \end{aligned} \tag{4.8}$$

where $\Delta = \omega - \omega_2$ is the detuning between the field and the atom. Similarly equation 4.6 may also be simplified into

$$\frac{dc_1}{dt} = -\frac{i\Omega}{2} \widetilde{c_2}\,. \tag{4.9}$$

To compute the probabilities of finding the two-level atom in state 1 and state 2, the expressions of the coefficients c_1 and $\widetilde{c_2}$ have to be first determined. First, the expression in equation 4.9 is rearranged into a simpler integral form. Both sides of the equation 4.9 are differentiated with respect to time to obtain

$$\frac{d^2c_1}{dt^2} = -\frac{i\Omega}{2}\frac{d\widetilde{c_2}}{dt}.$$

By substituting equation 4.8 into this expression, we therefore obtain

$$\frac{d^2c_1}{dt^2} = -\frac{i\Omega}{2}\left(i\Delta\widetilde{c_2} - \frac{i\Omega}{2}c_1\right).$$

Then equation 4.9 is substituted into the expression to replace $\widetilde{c_2}$ and obtain

$$\begin{aligned}
\frac{d^2c_1}{dt^2} &= i\Delta\frac{dc_1}{dt} - \left(\frac{\Omega}{2}\right)^2 c_1 \\
\frac{d^2c_1}{dt^2} - i\Delta\frac{dc_1}{dt} + \left(\frac{\Omega}{2}\right)^2 c_1 &= 0 \\
\left(\frac{d^2}{dt^2} - i\Delta\frac{d}{dt} + \left(\frac{\Omega}{2}\right)^2\right)c_1 &= 0 \qquad (4.10) \\
\left[\left(\frac{d}{dt} - \frac{i\Delta}{2}\right)^2 + \left(\frac{\Omega}{2}\right)^2 + \left(\frac{\Delta}{2}\right)^2\right]c_1 &= 0\,.
\end{aligned}$$

Suppose $\widetilde{\Omega} = \sqrt{\Omega^2 + \Delta^2}$, we then have

$$\left(\frac{d}{dt} - \frac{i\Delta}{2} + \frac{i\widetilde{\Omega}}{2}\right)\left(\frac{d}{dt} - \frac{i\Delta}{2} - \frac{i\widetilde{\Omega}}{2}\right)c_1 = 0\,. \qquad (4.11)$$

Now that a simpler expression for c_1 is obtained, we move on to rearrange the expression for $\widetilde{c_2}$. First, both sides of equation 4.8 are differentiated with respect to time to obtain

$$\frac{d^2\widetilde{c_2}}{dt^2} = i\Delta\frac{d\widetilde{c_2}}{dt} - i\frac{\Omega}{2}\frac{dc_1}{dt}.$$

Then we substitute equations 4.8 and 4.9 into the expression so that

$$\frac{d^2\widetilde{c_2}}{dt^2} = i\Delta\left(i\Delta\widetilde{c_2} - \frac{i\Omega}{2}c_1\right) - \frac{i\Omega}{2}\left(-\frac{i\Omega}{2}\widetilde{c_2}\right).$$

Following that, equation 4.8 is substituted into the expression to replace c_1, we therefore obtain

$$\frac{d^2\widetilde{c_2}}{dt^2} = -\Delta^2\widetilde{c_2} + i\Delta\frac{d\widetilde{c_2}}{dt} + \Delta^2\widetilde{c_2} - \left(\frac{\Omega}{2}\right)^2\widetilde{c_2}$$

$$\frac{d^2\widetilde{c_2}}{dt^2} - i\Delta\frac{d\widetilde{c_2}}{dt} + \left(\frac{\Omega}{2}\right)^2\widetilde{c_2} = 0$$

$$\left(\frac{d^2}{dt^2} - i\Delta\frac{d}{dt} + \left(\frac{\Omega}{2}\right)^2\right)\widetilde{c_2} = 0\,.$$

It is observed that the expression has the same form as equation 4.10, hence we may immediately deduce that it is equivalent to

$$\left(\frac{d}{dt} - \frac{i\Delta}{2} + \frac{i\widetilde{\Omega}}{2}\right)\left(\frac{d}{dt} - \frac{i\Delta}{2} - \frac{i\widetilde{\Omega}}{2}\right)\widetilde{c_2} = 0\,. \tag{4.12}$$

Now that the equations involving c_1 and $\widetilde{c_2}$ are expressed in suggestive forms, we proceed to solve for the coefficients. Firstly, we attempt to find c_1 by solving the equation 4.11 such that

$$\frac{dc_1}{dt} - \frac{i\Delta}{2}c_1 \pm \frac{i\widetilde{\Omega}}{2}c_1 = 0$$

$$\frac{dc_1}{dt} = \left(\frac{i\Delta}{2} \mp \frac{i\widetilde{\Omega}}{2}\right)c_1$$

$$\int\frac{dc_1}{c_1} = \int\left(\frac{i\Delta}{2} \mp \frac{i\widetilde{\Omega}}{2}\right)dt$$

$$\ln(c_1) = \left(\frac{i\Delta}{2} \mp \frac{i\widetilde{\Omega}}{2}\right)t + k$$

$$c_1 = Kexp\left(\frac{i\Delta}{2}t\right)exp\left(\mp\frac{i\widetilde{\Omega}}{2}t\right),$$

where k and $K = \exp(k)$ are constants. It may be further simplified into

$$c_1(t) = exp\left(\frac{i\Delta}{2}t\right)\left[A_1\cos\frac{1}{2}\widetilde{\Omega}t + B_1\sin\frac{1}{2}\widetilde{\Omega}t\right]. \quad (4.13)$$

Similarly $\widetilde{c_2}$ can be found by solving the equation 4.12 so that we obtain

$$\widetilde{c_2}(t) = exp\left(\frac{i\Delta}{2}t\right)\left[A_2\cos\frac{1}{2}\widetilde{\Omega}t + B_2\sin\frac{1}{2}\widetilde{\Omega}t\right]. \quad (4.14)$$

A_1, A_2, B_1 and B_2 are terms that need to be determined. When *t = 0*, obviously

$$A_1 = c_1(0), \quad (4.15)$$
$$A_2 = \widetilde{c_2}(0) = c_2(0). \quad (4.16)$$

To solve for the remaining terms, we differentiate equation 4.13 with respect to time to yield

$$\frac{dc_1(t)}{dt} = \frac{i\Delta}{2}exp\left(\frac{i\Delta}{2}t\right)\left[A_1\cos\frac{1}{2}\widetilde{\Omega t} + B_1\sin\frac{1}{2}\widetilde{\Omega t}\right] + exp\left(\frac{i\Delta}{2}t\right)\frac{1}{2}\widetilde{\Omega}\left[-A_1\sin\frac{1}{2}\widetilde{\Omega}t + B_1\cos\frac{1}{2}\widetilde{\Omega}t\right].$$

If we equate this expression to equation 4.9 and let time *t = 0*, the expression

$$-\frac{i\Omega}{2}c_2(0) = \frac{i\Delta}{2}A_1 + \frac{1}{2}\widetilde{\Omega}B_1$$

may be obtained. We then substitute in equation 4.15 and rearrange the equation such that

$$B_1 = -\frac{i\Omega}{\widetilde{\Omega}} c_2(0) - \frac{i\Delta}{\widetilde{\Omega}} c_1(0)$$

$$B_1 = -\frac{i}{\widetilde{\Omega}} [\Omega c_2(0) + \Delta c_1(0)]. \quad (4.17)$$

In order to gain the solution to the last term B_2, we repeat the same process by differentiating equation 4.14 with respect to time and equating it to equation 4.8, at the same time impose the initial condition time *t = 0* to yield

$$i\Delta c_2(0) - \frac{i\Omega}{2} c_1(0) = \frac{i\Delta}{2} A_2 + \frac{1}{2}\widetilde{\Omega} B_2 \, .$$

We now substitute in equation 4.16 and rearrange the equation to obtain

$$B_2 = \frac{i\Delta}{\widetilde{\Omega}} c_2(0) - \frac{i\Omega}{\widetilde{\Omega}} c_1(0)$$

$$B_2 = \frac{i}{\widetilde{\Omega}} [\Delta c_2(0) + \Omega c_1(0)] \, . \quad (4.18)$$

Finally, we substitute the equations from 4.15 to 4.18 into equation 4.13 and 4.14; the final expressions for the coefficients are obtained to be

$$c_1(t) = exp\left(\frac{i\Delta}{2} t\right) \left[c_1(0) \cos\frac{1}{2}\widetilde{\Omega} t - \frac{i}{\widetilde{\Omega}} [\Omega c_2(0) + \Delta c_1(0)] \, \sin\frac{1}{2}\widetilde{\Omega} t \right], \quad (4.19)$$

and

$$c_2(t) = exp\left(\frac{i\Delta}{2} t\right) \left[c_2(0) \cos\frac{1}{2}\widetilde{\Omega} t + \frac{i}{\widetilde{\Omega}} [\Delta c_2(0) + \Omega c_1(0)] \sin\frac{1}{2}\widetilde{\Omega} t \right]. \quad (4.20)$$

4.1.5 Resonant case

In resonant case, $\omega = \omega_2$ that is, $\Delta = 0$. This also implies that $\widetilde{\Omega} = \Omega$. Applying these conditions to equation 4.19 and 4.20, the two simplified expressions can then be obtained as

$$c_1(t) = c_1(0)\cos\frac{1}{2}\Omega t - ic_2(0)\sin\frac{1}{2}\Omega t, \tag{4.21}$$

$$c_2(t) = c_2(0)\cos\frac{1}{2}\Omega t + ic_1(0)\sin\frac{1}{2}\Omega t. \tag{4.22}$$

Suppose the atom is initially unexcited, that is $c_1(0) = 1$ and $c_2(0) = 0$, then the probabilities of finding the atom in state 1 and state 2 are

$$P_1(t) = |c_1(t)|^2 = \cos^2\frac{1}{2}\Omega t, \tag{4.23}$$

$$P_2(t) = |c_2(t)|^2 = \sin^2\frac{1}{2}\Omega t, \tag{4.24}$$

respectively.

The probability expressions in equations 4.23 and 4.24 are plotted in MATLAB as depicted in figure 4.1 below. The probability of atom staying in each state is plotted against Ωt, where Ω is the Rabi frequency and t is time. For $P_2(t)$, the upward swings correspond to the absorption of light field energy by the atom to jump up to the excited state whereas the downward trends correspond to the stimulated emission whereby the atom jumps back down to the ground state accompanied by the emission of light. In contrast, the trends in $P_1(t)$ indicate the exact opposite processes. The shapes of both $P_1(t)$ and $P_2(t)$ graphs are both in sinusoidal waveform, and it is observed that $P_1(t) + P_2(t) = 1$ holds for all Ωt, indicating the conservation of probability. Such cyclic nature is also known as the Rabi oscillation. Another observation made is that the populations of both ground state and excited state oscillate between 0 and 1 with a period of $T = \frac{2\pi}{\Omega}$. This means that if a laser light is shined upon the atom for half a period of time, that is $\frac{T}{2} = \frac{\pi}{\Omega}$, a population inversion can be achieved. However, this also poses a problem such that if the laser light is shined on the atom to achieve population inversion (*i.e.* the atom is in excited state), then the laser light is switched off and the atom will stay excited for an indefinite amount of time. This violates the experimental observation that atom should always jump back down to the lower energy level by spontaneous emission, provided that there are available state in the ground state.

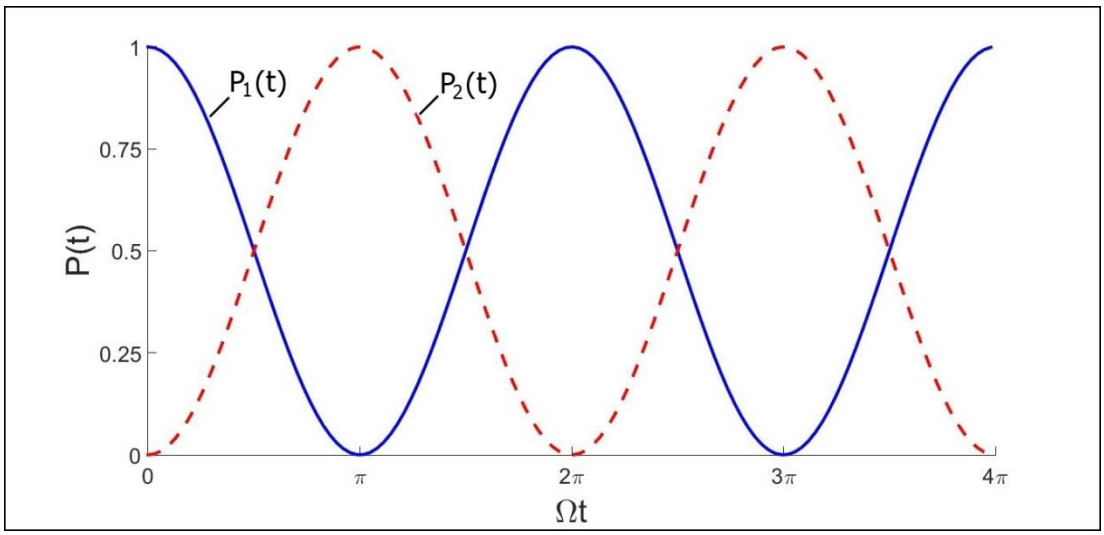

Figure 4.1: Populations in the ground state and the excited state for resonant case.

4.1.6 Near resonant case

We now proceed to employ the similar condition of initially unexcited atom from the previous section, so that the corresponding coefficients are now

$$c_1(t) = exp\left(\frac{i\Delta}{2}t\right)\left[\cos\frac{1}{2}\widetilde{\Omega}t - \frac{i\Delta}{\widetilde{\Omega}}\sin\frac{1}{2}\widetilde{\Omega}t\right], \tag{4.25}$$

$$c_2(t) = exp\left(\frac{i\Delta}{2}t\right)\left[\frac{i\Omega}{\widetilde{\Omega}}\sin\frac{1}{2}\widetilde{\Omega}t\right]. \tag{4.26}$$

Therefore the probabilities of finding the atom to reside in state 1 and state 2 are

$$P_1(t) = |c_1(t)|^2 = \cos^2\frac{1}{2}\widetilde{\Omega}t + \frac{\Delta^2}{\widetilde{\Omega}^2}\sin^2\frac{1}{2}\widetilde{\Omega}t, \tag{4.27}$$

$$P_2(t) = |c_2(t)|^2 = \frac{\Omega^2}{\widetilde{\Omega}^2}\sin^2\frac{1}{2}\widetilde{\Omega}t, \tag{4.28}$$

respectively.

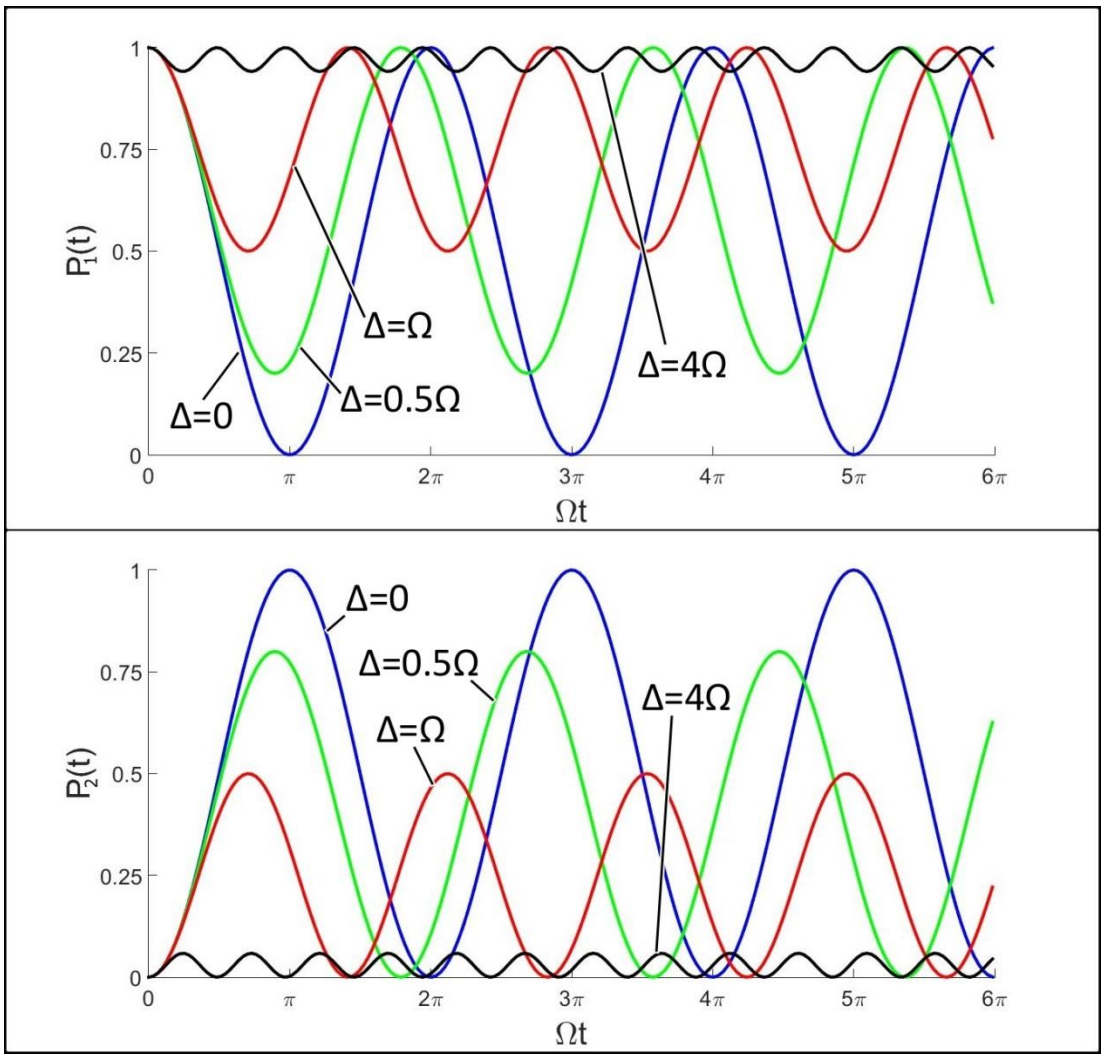

Figure 4.2: Populations in ground state (top) and excited state (bottom) for near resonant case.

Figure 4.2 illustrates the graph plot of ground state and excited state populations for near resonant case with different detuning Δ. At first glance, the populations of excited state and ground state are direct inversion of each other for all Δ, but the conservation of probability is no longer valid in this case. Nevertheless it is sufficient to focus the discussion solely on the excited state. Figure 4.2 shows that even with different detuning, the population exhibits similar smooth sinusoidal oscillation. In contrast, there are two key differences in the population oscillation with different detuning; as the detuning gets higher, both (1) the period and (2) the amplitude decreases. Interestingly, the lower amplitude indicates lower probability for the atom to jump up to the excited state when the field is out of resonance with the atom, despite the fact that the field may carry substantially more energy to

transfer to the atom. Nonetheless, in this two-level model, it is assumed that the detuning is sufficiently small so that higher energy levels are irrelevant.

4.2 General Approach to Quantum Mechanical Treatment

The following few sections shall demonstrate the solution for the full quantum mechanical treatment of the light-matter interaction. In this treatment, not only that the two-level atom is treated quantum mechanically, the single-mode light field is expressed as quantised field state. The general strategy of this treatment is to first obtain the total Hamiltonian of the joint system (i.e. the sum of atomic Hamiltonian, field Hamiltonian and interaction Hamiltonian), then transforms it from Schrodinger picture to interaction picture. The Hamiltonian obtained is then used to solve the Schrodinger equation to obtain the wavefunction of the joint system.

4.3 Unitary Transformation on Hamiltonian

4.3.1 Hamiltonian in Schrodinger Picture

Suppose a two-state system is interacting with discrete photons, the Hamiltonian of the quantum system in Schrodinger picture may be expressed in the form

$$\begin{aligned} \hat{H}_S &= \hat{H}_{S,A} + \hat{H}_{S,F} + \hat{H}_{S,int} \\ &= \hat{H}_{S,0} + \hat{H}_{S,int} \ , \end{aligned} \tag{4.29}$$

where $\hat{H}_{S,0} = \hat{H}_{S,A} + \hat{H}_{S,F}$ is the free term of the Hamiltonian, $\hat{H}_{S,int}$ is the interaction Hamiltonian, $\hat{H}_{S,A}$ is the atomic Hamiltonian and $\hat{H}_{S,F}$ is the field Hamiltonian.

The single-mode field Hamiltonian can be obtained through quantisation procedure on the photon field which is shown in section 2.3 as

$$\hat{H}_{S,F} = \hbar\omega\hat{a}_+\hat{a}_- + \frac{1}{2}\hbar\omega.$$

The atomic Hamiltonian of a two-level system can be formulated as

$$\hat{H}_{S,A}(|1\rangle\langle 1| + |2\rangle\langle 2|) = E_1|1\rangle\langle 1| + E_2|2\rangle\langle 2|,$$

where $|1\rangle\langle 1| + |2\rangle\langle 2|$ is complete and its density matrix form is equivalent to that of an identity matrix, such that

$$|1\rangle\langle 1| + |2\rangle\langle 2| = \begin{pmatrix} 1 & 0 \\ 0 & 1 \end{pmatrix} = \hat{I}.$$

Furthermore, $E_1 = \hbar\omega_1$ and $E_2 = \hbar\omega_2$, therefore the equation becomes

$$\widehat{H}_{S,A}\hat{I} = \hbar\omega_1|1\rangle\langle 1| + \hbar\omega_2|2\rangle\langle 2|\,,$$

and $\widehat{H}_{S,A}$ may be rewritten in the form of

$$\widehat{H}_{S,A} = \begin{pmatrix} \hbar\omega_2 & 0 \\ 0 & \hbar\omega_1 \end{pmatrix}.$$

It may be useful to re-express $\widehat{H}_{S,A}$ in terms of Pauli matrices, so that it is in a more suggestive form. We suppose $\widehat{H}_{S,A} = a_1\hat{I} + a_2\hat{\sigma}_z$, such that

$$\begin{pmatrix} \hbar\omega_2 & 0 \\ 0 & \hbar\omega_1 \end{pmatrix} = a_1\begin{pmatrix} 1 & 0 \\ 0 & 1 \end{pmatrix} + a_2\begin{pmatrix} 1 & 0 \\ 0 & -1 \end{pmatrix}.$$

By solving the simultaneous equation, the coefficients can be obtained as

$$a_1 = \frac{1}{2}\hbar(\omega_2 + \omega_1),$$
$$a_2 = \frac{1}{2}\hbar(\omega_2 - \omega_1).$$

Hence the atomic Hamiltonian in Schrodinger picture can be expressed as

$$\widehat{H}_{S,A} = \frac{1}{2}\hbar(\omega_2 + \omega_1)\hat{I} + \frac{1}{2}\hbar(\omega_2 - \omega_1)\hat{\sigma}_z. \tag{4.30}$$

Next, we proceed to find the expression for the interaction Hamiltonian. In the photon-atom interaction, the electric-dipole interaction dominates. The dipole operator can be expressed in the form

$$\widehat{\boldsymbol{d}} = \boldsymbol{d}^*\hat{\sigma}_+ + \boldsymbol{d}\hat{\sigma}_-,$$

so that $\widehat{\boldsymbol{d}}|1\rangle = \boldsymbol{d}^*|2\rangle$ and $\widehat{\boldsymbol{d}}|2\rangle = \boldsymbol{d}|1\rangle$. For simplicity, the dipole vectors are taken to be real, so that $\boldsymbol{d} = \boldsymbol{d}^*$, then the interaction Hamiltonian in Schrodinger picture is

$$\widehat{H}_{S,int} = -\boldsymbol{d}(\hat{\sigma}_+ + \hat{\sigma}_-) \cdot \boldsymbol{E}.$$

From equation 2.33 in section 2.3, the $\boldsymbol{E}$ field of a single mode field is obtained to be

$$\boldsymbol{E}(\boldsymbol{r}, t) = \frac{1}{\sqrt{\varepsilon_0 V}}\dot{\hat{q}}(t)\boldsymbol{v}(\boldsymbol{r}),$$

where $\dot{\hat{q}} = \frac{\hat{p}}{m} = i\sqrt{\frac{\hbar\omega}{2}}(\hat{a}_+ - \hat{a}_-)$. We then substitute in the $\boldsymbol{E}$ field equation into the interaction Hamiltonian so that

$$\begin{aligned}\widehat{H}_{S,int} &= -\boldsymbol{d}(\hat{\sigma}_+ + \hat{\sigma}_-) \cdot \boldsymbol{v}(\boldsymbol{r}) i\sqrt{\frac{\hbar\omega}{2\varepsilon_0 V}}(\hat{a}_+ - \hat{a}_-) \\ &= i\hbar\boldsymbol{d} \cdot \boldsymbol{v}(\boldsymbol{r})\sqrt{\frac{\omega}{2\hbar\varepsilon_0 V}}(\hat{\sigma}_+ + \hat{\sigma}_-)(\hat{a}_- - \hat{a}_+) \\ &= i\hbar\lambda(\hat{\sigma}_+ + \hat{\sigma}_-)(\hat{a}_- - \hat{a}_+), \end{aligned} \tag{4.31}$$

where $\lambda = \boldsymbol{d} \cdot \boldsymbol{v}(\boldsymbol{r})\sqrt{\frac{\omega}{2\hbar\varepsilon_0 V}}$ is the interaction strength. The total Hamiltonian in the Schrodinger picture can then be expressed in the form of

$$\begin{aligned}\widehat{H}_S = \frac{1}{2}\hbar(\omega_2 + \omega_1)\hat{I} + \frac{1}{2}\hbar(\omega_2 - \omega_1)\hat{\sigma}_z + \hbar\omega\hat{a}_+\hat{a}_- + \frac{1}{2}\hbar\omega \\ + i\hbar\lambda(\hat{\sigma}_+ + \hat{\sigma}_-)(\hat{a}_- - \hat{a}_+).\end{aligned}$$

4.3.2 Hamiltonian in Interaction Picture

The Hamiltonian in the interaction picture can be derived using the transformation relation in equation 2.31 which can be found in section 2.4.3 as

$$\begin{aligned}\widehat{H}_I &= i\hbar\frac{\partial\widehat{U}}{\partial t}\widehat{U}^\dagger + \widehat{U}\widehat{H}_S\widehat{U}^\dagger \\ &= i\hbar\frac{\partial\widehat{U}}{\partial t}\widehat{U}^\dagger + \widehat{U}\widehat{H}_{S,0}\widehat{U}^\dagger + \widehat{U}\widehat{H}_{S,int}\widehat{U}^\dagger. \end{aligned} \tag{4.32}$$

The unitary transformation and its time derivatives are in the forms of

$$\widehat{U} = \exp\left(\frac{i\widehat{H}_{S,U}t}{\hbar}\right), \tag{4.33}$$

$$\widehat{U}^\dagger = \exp\left(\frac{-i\widehat{H}_{S,U}t}{\hbar}\right), \tag{4.34}$$

$$\frac{\partial\widehat{U}}{\partial t} = \frac{i}{\hbar}\widehat{H}_{S,U}\exp\left(\frac{i\widehat{H}_{S,U}t}{\hbar}\right), \tag{4.35}$$

where $\widehat{H}_{S,U} = [\hbar(\omega_2 - \omega - \delta)]|1\rangle\langle 1| + [\hbar(\omega_2 - \delta)]|2\rangle\langle 2| + \hbar\omega\left(\hat{a}_+\hat{a}_- + \frac{1}{2}\right)$ is the free term of the joint system Hamiltonian, $\delta = \frac{\Delta}{2}$ and $\Delta = \omega_2 - \omega_1 - \omega$ is the detuning.

We now proceed to find the simplified expression of each term in equation 4.32. Firstly, the first term may be re-expressed as

$$\begin{aligned} i\hbar\frac{\partial\widehat{U}}{\partial t}\widehat{U}^\dagger &= i\hbar\left(\frac{i}{\hbar}\widehat{H}_{S,U}e^{\frac{i\widehat{H}_{S,U}t}{\hbar}}\right)\left(e^{\frac{-i\widehat{H}_{S,U}t}{\hbar}}\right) \\ &= -\widehat{H}_{S,U} \\ &= -\hbar\begin{bmatrix}\omega_2 - \delta & 0 \\ 0 & \omega_2 - \omega - \delta\end{bmatrix} - \hbar\omega\left(\hat{a}_+\hat{a}_- + \frac{1}{2}\right). \end{aligned}$$

Similarly, the second term may also be simplified as

$$\begin{aligned}\widehat{U}\widehat{H}_{S,0}\widehat{U}^{\dagger} &= \left(e^{\frac{i\widehat{H}_{S,U}t}{\hbar}}\right)\widehat{H}_{S,0}\left(e^{\frac{-i\widehat{H}_{S,U}t}{\hbar}}\right)\\ &= \widehat{H}_{S,0}\\ &= \hbar\begin{bmatrix}\omega_2 & 0\\ 0 & \omega_1\end{bmatrix} + \hbar\omega\left(\hat{a}_{+}\hat{a}_{-} + \frac{1}{2}\right).\end{aligned}$$

Hence the first two terms may be summed up so that

$$\begin{aligned}i\hbar\frac{\partial\widehat{U}}{\partial t}\widehat{U}^{\dagger} + \widehat{U}\widehat{H}_{S,0}\widehat{U}^{\dagger} &= \hbar\begin{bmatrix}\delta & 0\\ 0 & \omega + \omega_1 - \omega_2 + \delta\end{bmatrix}\\ &= \hbar\begin{bmatrix}\Delta/2 & 0\\ 0 & -\Delta/2\end{bmatrix}\\ &= \left(\frac{\hbar\Delta}{2}\right)\hat{\sigma}_z. \qquad (4.36)\end{aligned}$$

On the other hand, the simplification process of the third term is trickier. We first re-express the third term as

$$\begin{aligned}\widehat{U}\widehat{H}_{S,int}\widehat{U}^{\dagger} &= \left(e^{\frac{i\widehat{H}_{S,U}t}{\hbar}}\right)\left(i\hbar\lambda(\hat{\sigma}_{+} + \hat{\sigma}_{-})(\hat{a}_{-} - \hat{a}_{+})\right)\left(e^{\frac{-i\widehat{H}_{S,U}t}{\hbar}}\right)\\ &= \left(e^{\frac{i(\widehat{H}_{S,A}+\widehat{H}_{S,F})t}{\hbar}}\right)\left(i\hbar\lambda(\hat{\sigma}_{+} + \hat{\sigma}_{-})(\hat{a}_{-} - \hat{a}_{+})\right)\left(e^{\frac{-i(\widehat{H}_{S,A}+\widehat{H}_{S,F})t}{\hbar}}\right),\end{aligned}$$

where $\widehat{H}_{S,A} = [\hbar(\omega_2 - \omega - \delta)]|1\rangle\langle 1| + [\hbar(\omega_2 - \delta)]|2\rangle\langle 2|$ is the atomic Hamiltonian and $\widehat{H}_{S,F} = \hbar\omega\left(\hat{a}_{+}\hat{a}_{-} + \frac{1}{2}\right)$ is the field Hamiltonian. Since the ladder operators $\hat{\sigma}_{+}$ and $\hat{\sigma}_{-}$ act only on $\widehat{H}_{S,A}$ whereas $\hat{a}_{+}$ and $\hat{a}_{-}$ act only on $\widehat{H}_{S,F}$, the third term can thus be rearranged and solved separately for both the atomic Hamiltonian and field Hamiltonian, such that

$$\widehat{U}\widehat{H}_{S,int}\widehat{U}^{\dagger} = i\hbar\lambda\left\{e^{\frac{i\widehat{H}_{S,A}t}{\hbar}}(\hat{\sigma}_{+} + \hat{\sigma}_{-})e^{\frac{-i\widehat{H}_{S,A}t}{\hbar}}\right\}\left\{e^{\frac{i\widehat{H}_{S,F}t}{\hbar}}(\hat{a}_{-} - \hat{a}_{+})e^{\frac{-i\widehat{H}_{S,F}t}{\hbar}}\right\}. \qquad (4.37)$$

To solve for the atomic Hamiltonian part of the factor, $\left\{e^{\frac{i\hat{H}_{S,A}t}{\hbar}}(\hat{\sigma}_+ + \hat{\sigma}_-)e^{\frac{-i\hat{H}_{S,A}t}{\hbar}}\right\}$, it is first noted that the atomic Hamiltonian can be expressed in matrix form as

$$\hat{H}_{S,A} = \begin{pmatrix} \hbar(\omega_2 - \delta) & 0 \\ 0 & \hbar(\omega_2 - \omega - \delta) \end{pmatrix}.$$

Therefore, by making use of the mathematical identity derived in section 2.5, its exponential takes the form of

$$e^{\frac{i\hat{H}_{S,A}t}{\hbar}} = \begin{pmatrix} e^{i(\omega_2-\delta)t} & 0 \\ 0 & e^{i(\omega_2-\omega-\delta)t} \end{pmatrix}.$$

Moreover, the ladder operators may also be represented in matrix form such that

$$\hat{\sigma}_+ = \begin{pmatrix} 0 & 1 \\ 0 & 0 \end{pmatrix},$$

and

$$\hat{\sigma}_- = \begin{pmatrix} 0 & 0 \\ 1 & 0 \end{pmatrix}.$$

Hence, we make use of these expressions of matrices to solve for the atomic Hamiltonian part of the factor, so that

$$\begin{aligned} &\left\{e^{\frac{i\hat{H}_{S,A}t}{\hbar}}(\hat{\sigma}_+ + \hat{\sigma}_-)e^{\frac{-i\hat{H}_{S,A}t}{\hbar}}\right\} \\ &= \begin{pmatrix} e^{i(\omega_2-\delta)t} & 0 \\ 0 & e^{i(\omega_2-\omega-\delta)t} \end{pmatrix}\begin{pmatrix} 0 & 1 \\ 1 & 0 \end{pmatrix}\begin{pmatrix} e^{-i(\omega_2-\delta)t} & 0 \\ 0 & e^{-i(\omega_2-\omega-\delta)t} \end{pmatrix} \\ &= \begin{pmatrix} 0 & e^{i\omega t} \\ e^{-i\omega t} & 0 \end{pmatrix} \\ &= e^{i\omega t}\hat{\sigma}_+ + e^{-i\omega t}\hat{\sigma}_-\,, \end{aligned} \tag{4.38}$$

where $\omega = \omega_2 - \omega_1 - \Delta$.

Next, we proceed to solve for the field Hamiltonian part of the factor, $\left\{e^{\frac{i\hat{H}_{S,F}t}{\hbar}}(\hat{a}_- - \hat{a}_+)e^{\frac{-i\hat{H}_{S,F}t}{\hbar}}\right\}$. The raising and lowering operators are first re-expressed into the form of

$$\hat{a}_+ = \sum_n \sqrt{n+1}|n+1\rangle\langle n|,$$
$$\hat{a}_- = \sum_n \sqrt{n+1}|n\rangle\langle n+1|,$$
$$\hat{a}_+\hat{a}_- = \sum_n (n+1)|n+1\rangle\langle n+1|.$$

Thus the field Hamiltonian can be re-expressed as

$$\hat{H}_{S,F} = \sum_n \hbar\omega\left((n+1)|n+1\rangle\langle n+1| + \frac{1}{2}\right).$$

Moreover, the field Hamiltonian part of the factor can be further separated into two parts for ease of derivation:

$$\left\{e^{\frac{i\hat{H}_{S,F}t}{\hbar}}(\hat{a}_- - \hat{a}_+)e^{\frac{-i\hat{H}_{S,F}t}{\hbar}}\right\} = \left\{e^{\frac{i\hat{H}_{S,F}t}{\hbar}}\hat{a}_-e^{\frac{-i\hat{H}_{S,F}t}{\hbar}}\right\} - \left\{e^{\frac{i\hat{H}_{S,F}t}{\hbar}}\hat{a}_+e^{\frac{-i\hat{H}_{S,F}t}{\hbar}}\right\}. \quad (4.39)$$

We first solve for the first term on the right side of equation 4.39 to yield

$$\left\{e^{\frac{i\hat{H}_{S,F}t}{\hbar}}\hat{a}_-e^{\frac{-i\hat{H}_{S,F}t}{\hbar}}\right\}$$
$$= \sum_m\sum_n\sum_r\left\{\exp\left(\frac{i\omega t}{2}\right)\exp\big(i\omega t(m+1)\big)\ |m+1\rangle\langle m+1|\right\}\left\{\sqrt{n+1}|n\rangle\langle n+1|\right\}\left\{\exp\left(\frac{-i\omega t}{2}\right)\exp\big(-i\omega t(r+1)\big)\ |r+1\rangle\langle r+1|\right\}.$$

Obviously due to the orthogonality property, $n = m + 1 = r$ must be true to produce any significant result. The expression may then be greatly simplified so that

$$\left\{e^{\frac{i\hat{H}_{S,F}t}{\hbar}}\hat{a}_{-}e^{\frac{-i\hat{H}_{S,F}t}{\hbar}}\right\}$$
$$= \sum_{n}\{\exp(i\omega t(n))\ |n\rangle\langle n|\}\{\sqrt{n+1}|n\rangle\langle n + 1|\}\{\exp(-i\omega t(n+1))\ |n+1\rangle\langle n+1|\}$$
$$= \sum_{n}\exp(-i\omega t)\sqrt{n+1}|n\rangle\langle n+1|$$
$$= \hat{a}_{-}e^{-i\omega t}. \tag{4.40}$$

Now, we proceed to solve for the second term on the right side of equation 4.39 such that

$$\left\{e^{\frac{i\hat{H}_{S,F}t}{\hbar}}\hat{a}_{+}e^{\frac{-i\hat{H}_{S,F}t}{\hbar}}\right\}$$
$$= \sum_{m}\sum_{n}\sum_{r}\left\{\exp\left(\frac{i\omega t}{2}\right)\exp(i\omega t(m+1))\ |m+1\rangle\langle m+1|\right\}\{\sqrt{n+1}|n + 1\rangle\langle n|\}\left\{\exp\left(\frac{-i\omega t}{2}\right)\exp(-i\omega t(r+1))\ |r+1\rangle\langle r+1|\right\}.$$

Obviously due to the orthogonality property, $n = m = r + 1$ must be true to produce any significant result. The expression may then be significantly simplified into

$$\left\{e^{\frac{i\hat{H}_{S,F}t}{\hbar}}\hat{a}_{+}e^{\frac{-i\hat{H}_{S,F}t}{\hbar}}\right\}$$
$$= \sum_{n}\{\exp(i\omega t(n+1))\ |n+1\rangle\langle n+1|\}\{\sqrt{n+1}|n + 1\rangle\}\{\exp(-i\omega t(n))\ |n\rangle\langle n|\}$$
$$= \sum_{n}\exp(i\omega t)\sqrt{n+1}|n+1\rangle\langle n|$$
$$= \hat{a}_{+}e^{i\omega t}. \tag{4.41}$$

Finally, we substitute in all the solutions for the Hamiltonian in interaction picture to obtain

$$\begin{aligned}\hat{H}_I &= i\hbar\frac{\partial\hat{U}}{\partial t}\hat{U}^\dagger + \hat{U}\hat{H}_{S,0}\hat{U}^\dagger + \hat{U}\hat{H}_{S,int}\hat{U}^\dagger \\ &= -\hat{H}_{S,0} + \hat{H}_{S,0} + i\hbar\lambda\left(e^{i\omega t}\hat{\sigma}_+ + e^{-i\omega t}\hat{\sigma}_-\right)\left(\hat{a}_- e^{-i\omega t} - \hat{a}_+ e^{i\omega t}\right) \\ &= i\hbar\lambda\left(\hat{\sigma}_+\hat{a}_- - \hat{\sigma}_-\hat{a}_+ - \hat{\sigma}_+\hat{a}_+ e^{2i\omega t} + \hat{\sigma}_-\hat{a}_- e^{-2i\omega t}\right). \end{aligned} \quad (4.42)$$

By applying rotating-wave approximation to remove the fast rotating terms, the Hamiltonian in interaction picture can be simplified into

$$\hat{H}_I = \frac{\hbar\Delta}{2}\hat{\sigma}_z - i\hbar\lambda(\hat{\sigma}_+\hat{a}_- - \hat{\sigma}_-\hat{a}_+). \quad (4.43)$$

The physical consequences of equation 4.43 are obvious: $\hat{\sigma}_+\hat{a}_-$ term refers to the atom absorbing a photon to jump to the excited state and $\hat{\sigma}_-\hat{a}_+$ term refers to the atom releasing a photon while jumping down to the ground state. Nevertheless this is not the sole possible form of interaction. Alternatively the atom may absorb k number of photons to be excited and similarly releases k number of photons when it is de-excited. The solution to such case can be easily extended to take the form

$$\hat{H}_I = \frac{\hbar\Delta}{2}\hat{\sigma}_z - i\hbar\lambda(\hat{\sigma}_+\hat{a}_-^k - \hat{\sigma}_-\hat{a}_+^k). \quad (4.44)$$

4.4 Probability Functions

4.4.1 Probability Function of Single-Photon Model

In this model, it is assumed that the atom absorbs single photon to be excited from the ground state to the excited state. Given a two-state system described by wavefunction

$$|\Psi_I(t)\rangle = \sum_{n=0}^{\infty} c_{1,n}(t)\,|1\rangle|n\rangle + c_{2,n}(t)\,|2\rangle|n\rangle, \quad (4.45)$$

where $c_{1,n}$ and $c_{2,n}$ are the only factors that carry the time dependence in the wavefunction. The atomic states $|1\rangle$ and $|2\rangle$, and the photon states $|n\rangle$ are time independent in this case. Therefore the Schrodinger equation in interaction picture is given as

$$-\frac{i}{\hbar}\hat{H}_I|\Psi_I(t)\rangle = \frac{\partial}{\partial t}|\Psi_I(t)\rangle. \tag{4.46}$$

For the right-hand side of equation 4.46, we can simply differentiate the wavefunction to yield

$$\begin{aligned}\frac{\partial}{\partial t}|\Psi_I(t)\rangle &= \frac{\partial}{\partial t}\sum_{n=0}^{\infty} c_{1,n}(t)\,|1\rangle|n\rangle + c_{2,n}(t)\,|2\rangle|n\rangle \\ &= \sum_{n=0}^{\infty} \dot{c}_{1,n}(t)\,|1\rangle|n\rangle + \dot{c}_{2,n}(t)\,|2\rangle|n\rangle\,.\end{aligned}$$

On the other hand, the left-hand side of equation 4.46 may be re-expressed in the form of

$$-\frac{i}{\hbar}\hat{H}_I|\Psi_I(t)\rangle = \frac{-i\Delta}{2}\hat{\sigma}_z|\Psi_I(t)\rangle - \lambda(\hat{\sigma}_+\hat{a}_- - \hat{\sigma}_-\hat{a}_+)|\Psi_I(t)\rangle.$$

By solving the first term, we obtain

$$\begin{aligned}\frac{-i\Delta}{2}\hat{\sigma}_z|\Psi_I(t)\rangle &= \left(\frac{i\Delta}{2}|1\rangle\langle 1| - \frac{i\Delta}{2}|2\rangle\langle 2|\right)\left(\sum_{n=0}^{\infty} c_{1,n}(t)\,|1\rangle|n\rangle + c_{2,n}(t)\,|2\rangle|n\rangle\right) \\ &= \sum_{n=0}^{\infty}\frac{i\Delta}{2}c_{1,n}(t)\,|1\rangle|n\rangle - \frac{i\Delta}{2}c_{2,n}(t)\,|2\rangle|n\rangle.\end{aligned}$$

Similarly, solving the second term yields

$$-\lambda(\hat{\sigma}_+\hat{a}_- - \hat{\sigma}_-\hat{a}_+)|\Psi_I(t)\rangle$$

$$= -\lambda(\hat{\sigma}_+\hat{a}_- - \hat{\sigma}_-\hat{a}_+)\left(\sum_{n=0}^{\infty} c_{1,n}(t)\,|1\rangle|n\rangle + c_{2,n}(t)\,|2\rangle|n\rangle\right)$$

$$= -\lambda\sum_{n=0}^{\infty}\sqrt{n}\,c_{1,n}(t)\,|2\rangle|n-1\rangle + \lambda\sum_{n=0}^{\infty}\sqrt{n+1}\,c_{2,n}(t)\,|1\rangle|n+1\rangle$$

$$= -\lambda\sum_{n=-1}^{\infty}\sqrt{n+1}\,c_{1,n+1}(t)\,|2\rangle|n\rangle + \lambda\sum_{n=1}^{\infty}\sqrt{n}\,c_{2,n-1}(t)\,|1\rangle|n\rangle$$

$$= -\lambda\sum_{n=0}^{\infty}\sqrt{n+1}\,c_{1,n+1}(t)\,|2\rangle|n\rangle + \lambda\sum_{n=0}^{\infty}\sqrt{n}\,c_{2,n-1}(t)\,|1\rangle|n\rangle.$$

We may now combine the results of the two terms, so that the left-hand side of equation 4.46 becomes

$$-\frac{i}{\hbar}\hat{H}_I|\Psi_I(t)\rangle = \sum_{n=0}^{\infty}\frac{i\Delta}{2}c_{1,n}(t)\,|1\rangle|n\rangle - \frac{i\Delta}{2}c_{2,n}(t)\,|2\rangle|n\rangle$$

$$- \lambda\sum_{n=0}^{\infty}\sqrt{n+1}\,c_{1,n+1}(t)\,|2\rangle|n\rangle + \lambda\sum_{n=0}^{\infty}\sqrt{n}\,c_{2,n-1}(t)\,|1\rangle|n\rangle$$

$$= \sum_{n=0}^{\infty}\left(\frac{i\Delta}{2}c_{1,n}(t) + \lambda\sqrt{n}\,c_{2,n-1}(t)\right)|1\rangle|n\rangle$$

$$+ \sum_{n=0}^{\infty}\left(-\frac{i\Delta}{2}c_{2,n}(t) - \lambda\sqrt{n+1}\,c_{1,n+1}(t)\right)|2\rangle|n\rangle.$$

Comparing the coefficients on the two sides of equation 4.46, we obtain two expressions which are

$$\dot{c}_{1,n}(t) = \frac{i\Delta}{2}c_{1,n}(t) + \lambda\sqrt{n}\,c_{2,n-1}(t), \tag{4.47}$$

$$\dot{c}_{2,n}(t) = -\frac{i\Delta}{2}c_{2,n}(t) - \lambda\sqrt{n+1}\,c_{1,n+1}(t). \tag{4.48}$$

To maintain the consistency, we rewrite equation 4.48 into

$$\dot{c}_{2,n-1}(t) = -\frac{i\Delta}{2} c_{2,n-1}(t) - \lambda\sqrt{n}\, c_{1,n}(t). \tag{4.49}$$

The problem is therefore simplified into simple differential equations. Firstly, we differentiate both sides of equation 4.47 with respect to time to yield

$$\ddot{c}_{1,n}(t) = \frac{i\Delta}{2} \dot{c}_{1,n}(t) + \lambda\sqrt{n}\, \dot{c}_{2,n-1}(t). \tag{4.50}$$

Then, equation 4.49 is substituted into equation 4.50 so that

$$\ddot{c}_{1,n}(t) = \frac{i\Delta}{2} \dot{c}_{1,n}(t) \; - \frac{i\Delta}{2} \lambda\sqrt{n} c_{2,n-1}(t) - \lambda^2 n\, c_{1,n}(t). \tag{4.51}$$

To further simplify it, we substitute equation 4.47 into equation 4.51 to obtain

$$\begin{aligned} \ddot{c}_{1,n}(t) &= \frac{i\Delta}{2} \dot{c}_{1,n}(t) \; - \frac{i\Delta}{2} \dot{c}_{1,n}(t) - \frac{\Delta^2}{4} c_{1,n}(t) - \lambda^2 n\, c_{1,n}(t), \\ &= -\left(\lambda^2 n + \frac{\Delta^2}{4}\right) c_{1,n}(t) \\ &= -\left(\frac{\Omega_R}{2}\right)^2 c_{1,n}(t), \end{aligned}$$

where $\Omega_R = \lambda^2 n + \frac{\Delta^2}{4}$. The solution for this double differential equation is simply

$$c_{1,n}(t) = A sin\left(\frac{\Omega_R}{2} t\right) + B cos\left(\frac{\Omega_R}{2} t\right). \tag{4.52}$$

Besides that, we also perform similar procedure on equation 4.49 to yield the result for $c_{2,n-1}(t)$. We begin by first differentiating both sides of equation 4.49 with respect to time so that

$$\ddot{c}_{2,n-1}(t) = -\frac{i\Delta}{2} \dot{c}_{2,n-1}(t) - \lambda\sqrt{n}\, \dot{c}_{1,n}(t). \tag{4.53}$$

Then we substitute equation 4.47 into equation 4.53 to obtain the expression

$$\ddot{c}_{2,n-1}(t) = -\frac{i\Delta}{2}\dot{c}_{2,n-1}(t) - \lambda\sqrt{n}\,\frac{i\Delta}{2}c_{1,n}(t) - \lambda^2 n c_{2,n-1}(t). \tag{4.54}$$

To further simplify the equation, equation 4.49 is substituted into equation 4.54 such that

$$\begin{aligned}\ddot{c}_{2,n-1}(t) &= -\frac{i\Delta}{2}\dot{c}_{2,n-1}(t) + \frac{i\Delta}{2}\dot{c}_{2,n-1}(t) - \frac{\Delta^2}{4}c_{2,n-1}(t) - \lambda^2 n c_{2,n-1}(t)\\ &= -\left(\lambda^2 n + \frac{\Delta^2}{4}\right)c_{2,n-1}(t)\\ &= -\left(\frac{\Omega_R}{2}\right)^2 c_{2,n-1}(t),\end{aligned}$$

where $\Omega_R = \lambda^2 n + \frac{\Delta^2}{4}$. The solution for this double differential equation is therefore

$$c_{2,n-1}(t) = Csin\left(\frac{\Omega_R}{2}t\right) + Dcos\left(\frac{\Omega_R}{2}t\right). \tag{4.55}$$

Suppose the system is initially unexcited whereas the field is in linear superposition of number states, the initial composite state can therefore be represented as

$$|\Psi_I(0)\rangle = \sum_{n=0}^{\infty} a_n\,|1\rangle|n\rangle.$$

Thus when $t = 0$, we observe that

$$c_{1,n}(0) = B = a_n,$$

and

$$c_{2,n-1}(0) = D = 0.$$

Imposing these initial conditions into equations 4.52 and 4.55 allows us to obtain the expressions of

$$c_{1,n}(t) = Asin\left(\frac{\Omega_R}{2}t\right) + a_n cos\left(\frac{\Omega_R}{2}t\right), \tag{4.56}$$

$$c_{2,n-1}(t) = Csin\left(\frac{\Omega_R}{2}t\right). \tag{4.57}$$

We now further differentiate equation 4.56 with respect to time such that

$$\dot{c}_{1,n}(t) = A\frac{\Omega_R}{2}cos\left(\frac{\Omega_R}{2}t\right) - a_n\frac{\Omega_R}{2}sin\left(\frac{\Omega_R}{2}t\right).$$

The left-hand side of the expression can be replaced with equation 4.47 so that

$$\frac{i\Delta}{2}c_{1,n}(t) + \lambda\sqrt{n}\,c_{2,n-1}(t) = A\frac{\Omega_R}{2}cos\left(\frac{\Omega_R}{2}t\right) - a_n\frac{\Omega_R}{2}sin\left(\frac{\Omega_R}{2}t\right).$$

Now impose the initial condition again, we therefore obtain

$$\frac{i\Delta}{2}c_{1,n}(0) + \lambda\sqrt{n}\,c_{2,n-1}(0) = A\frac{\Omega_R}{2},$$

$$\frac{i\Delta}{2}a_n = A\frac{\Omega_R}{2},$$

$$A = \frac{i\Delta a_n}{\Omega_R}.$$

Similarly, we differentiate equation 4.57 with respect to time to obtain the expression

$$\dot{c}_{2,n-1}(t) = C\frac{\Omega_R}{2}cos\left(\frac{\Omega_R}{2}t\right).$$

The left-hand side of the equation can be replaced with equation 4.49 so that

$$-\frac{i\Delta}{2}c_{2,n-1}(t) - \lambda\sqrt{n}\,c_{1,n}(t) = C\frac{\Omega_R}{2}cos\left(\frac{\Omega_R}{2}t\right).$$

Now impose the initial condition again, we therefore obtain

$$-\frac{i\Delta}{2}c_{2,n-1}(0) - \lambda\sqrt{n}\,c_{1,n}(0) = C\frac{\Omega_R}{2}.$$

$$-a_n\lambda\sqrt{n} = C\frac{\Omega_R}{2},$$

$$C = \frac{-2a_n\lambda\sqrt{n}}{\Omega_R}.$$

Finally, the coefficients are obtained to be

$$c_{1,n}(t) = a_n\left\{\frac{i\Delta}{\Omega_R}sin\left(\frac{\Omega_R}{2}t\right) + cos\left(\frac{\Omega_R}{2}t\right)\right\}, \tag{4.58}$$

$$c_{2,n-1}(t) = a_n\left\{\frac{-2\lambda\sqrt{n}}{\Omega_R}sin\left(\frac{\Omega_R}{2}t\right)\right\}, \tag{4.59}$$

where $\Omega_R = \sqrt{\Delta^2 + 4\lambda^2 n}$.

Therefore the probability functions of state 1 (ground state) and state 2 (excited state) at any given time can be obtained by computing

$$P_1(t) = \sum_{n=0}^{\infty}\left|c_{1,n}(t)\right|^2,$$

$$P_2(t) = \sum_{n=0}^{\infty}\left|c_{2,n}(t)\right|^2,$$

respectively. Since the probabilities must be conserved, that is $P_1(t) + P_2(t) = 1$, the characteristics of the two probability curves are complement to each other. Hence it is sufficient to limit our studies to only state 1 (ground state).

Besides that, both resonant case $\Delta = 0$ and near resonant case $\Delta \neq 0$ are considered. Assuming resonance case, the probability function for state 1 is then given as

$$P_1(t) = \sum_{n=0}^{\infty} \left|c_{1,n}(t)\right|^2$$
$$= \sum_{n=0}^{\infty} |a_n|^2 \cos^2\left(\frac{\Omega_R}{2} t\right)$$
$$= \sum_{n=0}^{\infty} |a_n|^2 \cos^2\left(\lambda n^{1/2}\, t\right).$$

On the other hand, assuming near resonant case $\Delta \neq 0$, the probability function for state 1 is then given as

$$P_1(t) = \sum_{n=0}^{\infty} \left|c_{1,n}(t)\right|^2$$
$$= \sum_{n=0}^{\infty} |a_n|^2 \left(\cos^2\left(\frac{\Omega_R}{2} t\right) + \left(\frac{\Delta}{\Omega_R}\right)^2 \sin^2\left(\frac{\Omega_R}{2} t\right)\right).$$

where $\Omega_R = \sqrt{\Delta^2 + 4\lambda^2 n}$.

4.4.2 Probability Function of Multiple-Photon Model

In this section, the excitation of atom may absorb multiple photons. Similar to the previous section in 4.3.1, the initial wavefunction of the system is represented as

$$|\Psi_I(t)\rangle = \sum_{n=0}^{\infty} c_{1,n}(t)\, |1\rangle|n\rangle + c_{2,n}(t)\, |2\rangle|n\rangle, \tag{4.60}$$

where $c_{1,n}$ and $c_{2,n}$ are the only factors that carry the time dependence in the wavefunction. The atomic states $|1\rangle$ and $|2\rangle$, and the photon states $|n\rangle$ are time independent in this case. By solving the Schrodinger equation in interaction picture, we obtain

$$-\frac{i}{\hbar} \hat{H}_I |\Psi_I(t)\rangle = \frac{\partial}{\partial t} |\Psi_I(t)\rangle. \tag{4.61}$$

Firstly, the right-hand side of equation 4.61 is derived to be in the form of

$$\frac{\partial}{\partial t}|\Psi_I(t)\rangle = \frac{\partial}{\partial t}\sum_{n=0}^{\infty} c_{1,n}(t)\,|1\rangle|n\rangle + c_{2,n}(t)\,|2\rangle|n\rangle$$
$$= \sum_{n=0}^{\infty} \dot{c}_{1,n}(t)\,|1\rangle|n\rangle + \dot{c}_{2,n}(t)\,|2\rangle|n\rangle.$$

On the other hand, the left-hand side of equation 4.61 can be re-expressed as

$$-\frac{i}{\hbar}\hat{H}_I|\Psi_I(t)\rangle = \frac{-i\Delta}{2}\hat{\sigma}_z|\Psi_I(t)\rangle - \lambda(\hat{\sigma}_+\hat{a}_-^k - \hat{\sigma}_-\hat{a}_+^k)|\Psi_I(t)\rangle.$$

We proceed by first solving the first term such that

$$\frac{-i\Delta}{2}\hat{\sigma}_z|\Psi_I(t)\rangle = \left(\frac{i\Delta}{2}|1\rangle\langle 1| - \frac{i\Delta}{2}|2\rangle\langle 2|\right)\left(\sum_{n=0}^{\infty} c_{1,n}(t)\,|1\rangle|n\rangle + c_{2,n}(t)\,|2\rangle|n\rangle\right)$$
$$= \sum_{n=0}^{\infty}\frac{i\Delta}{2}c_{1,n}(t)\,|1\rangle|n\rangle - \frac{i\Delta}{2}c_{2,n}(t)\,|2\rangle|n\rangle.$$

Next, we proceed to solve the second term to yield

$$-\lambda(\hat{\sigma}_+\hat{a}_-^k - \hat{\sigma}_-\hat{a}_+^k)|\Psi_I(t)\rangle$$
$$= -\lambda(\hat{\sigma}_+\hat{a}_-^k - \hat{\sigma}_-\hat{a}_+^k)\left(\sum_{n=0}^{\infty} c_{1,n}(t)\,|1\rangle|n\rangle + c_{2,n}(t)\,|2\rangle|n\rangle\right)$$
$$= -\lambda\sum_{n=0}^{\infty}\sqrt{n}\,\sqrt{n-1}\,\ldots\sqrt{n-k+1}c_{1,n}(t)\,|2\rangle|n-k\rangle$$
$$+\lambda\sum_{n=0}^{\infty}\sqrt{n+1}\,\sqrt{n+2}\,\ldots\sqrt{n+k}c_{2,n}(t)\,|1\rangle|n+k\rangle$$
$$= -\lambda\sum_{n=-k}^{\infty}\sqrt{n+k}\,\sqrt{n+k-1}\,\ldots\sqrt{n+1}\,c_{1,n+k}(t)\,|2\rangle|n\rangle$$
$$+\lambda\sum_{n=k}^{\infty}\sqrt{n-k+1}\,\sqrt{n-k+2}\,\ldots\sqrt{n}\,c_{2,n-k}(t)\,|1\rangle|n\rangle$$

$$= -\lambda \sum_{n=0}^{\infty} \sqrt{n+k}\,\sqrt{n+k-1}\,\ldots\sqrt{n+1}\,c_{1,n+k}(t)\,|2\rangle|n\rangle + \lambda \sum_{n=0}^{\infty} \sqrt{n-k+1}\,\sqrt{n-k+2}\,\ldots\sqrt{n}\,c_{2,n-k}(t)\,|1\rangle|n\rangle.$$

By combining the two terms, the left-hand side of equation 4.61 becomes

$$-\frac{i}{\hbar}\widehat{H}_I|\Psi_I(t)\rangle = \sum_{n=0}^{\infty} \frac{i\Delta}{2} c_{1,n}(t)\,|1\rangle|n\rangle - \frac{i\Delta}{2} c_{2,n}(t)\,|2\rangle|n\rangle - \lambda \sum_{n=0}^{\infty} \sqrt{n+k}\,\sqrt{n+k-1}\,\ldots\sqrt{n+1}\,c_{1,n+k}(t)\,|2\rangle|n\rangle + \lambda \sum_{n=0}^{\infty} \sqrt{n-k+1}\,\sqrt{n-k+2}\,\ldots\sqrt{n}\,c_{2,n-k}(t)\,|1\rangle|n\rangle$$

$$-\frac{i}{\hbar}\widehat{H}_I|\Psi_I(t)\rangle = \sum_{n=0}^{\infty} \left(\frac{i\Delta}{2} c_{1,n}(t) + \lambda\sqrt{n-k+1}\,\sqrt{n-k+2}\,\ldots\sqrt{n}\,c_{2,n-k}(t) \right) |1\rangle|n\rangle + \sum_{n=0}^{\infty} \left(-\frac{i\Delta}{2} c_{2,n}(t) - \lambda\sqrt{n+k}\,\sqrt{n+k-1}\,\ldots\sqrt{n+1}\,c_{1,n+k}(t) \right) |2\rangle|n\rangle.$$

Through comparisons between the two sides of equation 4.61, we obtain two expressions which are

$$\dot{c}_{1,n}(t) = \frac{i\Delta}{2} c_{1,n}(t) + \lambda\sqrt{n-k+1}\,\sqrt{n-k+2}\,\ldots\sqrt{n}\,c_{2,n-k}(t), \tag{4.62}$$

$$\dot{c}_{2,n}(t) = -\frac{i\Delta}{2} c_{2,n}(t) - \lambda\sqrt{n+k}\,\sqrt{n+k-1}\,\ldots\sqrt{n+1}\,c_{1,n+k}(t). \tag{4.63}$$

To maintain the consistency, equation 4.63 can be rewritten as

$$\dot{c}_{2,n-k}(t) = -\frac{i\Delta}{2} c_{2,n-k}(t) - \lambda\sqrt{n-k+1}\,\sqrt{n-k+2}\,\ldots\sqrt{n}\,c_{1,n}(t). \tag{4.64}$$

We let $n' = \sqrt{n-k+1}\,\sqrt{n-k+2}\,...\sqrt{n}$, so that equations 4.62 and 4.64 can be rewritten into simpler form as follows,

$$\dot{c}_{1,n}(t) = \frac{i\Delta}{2} c_{1,n}(t) + \lambda n'\, c_{2,n-k}(t), \tag{4.65}$$

$$\dot{c}_{2,n-k}(t) = -\frac{i\Delta}{2} c_{2,n-k}(t) - \lambda n'\, c_{1,n}(t). \tag{4.66}$$

Remarkably equations 4.65 and 4.66 are very similar to equations 4.47 and 4.49 respectively. There are only two distinctions between the two sets of equations: (a) the coefficient term $n-1$ is replaced with $n-k$ and (b) the constant $\sqrt{n}$ is replaced with n'. Therefore, the exact same derivation process in section 4.4.1 may be carried out and the results are simply

$$c_{1,n}(t) = a_n \left\{ \frac{i\Delta}{\Omega_R} sin\left(\frac{\Omega_R}{2} t\right) + cos\left(\frac{\Omega_R}{2} t\right) \right\}, \tag{4.67}$$

$$c_{2,n-k}(t) = a_n \left\{ \frac{-2\lambda n'}{\Omega_R} sin\left(\frac{\Omega_R}{2} t\right) \right\}, \tag{4.68}$$

where $\Omega_R = \sqrt{\Delta^2 + 4\lambda^2 n'^2}$ and $n' = \sqrt{n-k+1}\,\sqrt{n-k+2}\,...\sqrt{n}$.

Finally, if we assume resonance case, the probability function for state 1 is therefore

$$\begin{aligned} P_1(t) &= \sum_{n=0}^{\infty} \left| c_{1,n}(t) \right|^2 \\ &= \sum_{n=0}^{\infty} |a_n|^2 \cos^2\left(\frac{\Omega_R}{2} t\right) \\ &= \sum_{n=0}^{\infty} |a_n|^2 \cos^2(\lambda n'\, t). \end{aligned}$$

On the other hand, assuming near resonant case, the probability function for state 1 is therefore given as

$$P_1(t) = \sum_{n=0}^{\infty} \left|c_{1,n}(t)\right|^2$$
$$= \sum_{n=0}^{\infty} |a_n|^2 \left(\cos^2\left(\frac{\Omega_R}{2}t\right) + \left(\frac{\Delta}{\Omega_R}\right)^2 \sin^2\left(\frac{\Omega_R}{2}t\right)\right).$$

where $\Omega_R = \sqrt{\Delta^2 + 4\lambda^2 n'^2}$ and $n' = \sqrt{n-k+1}\,\sqrt{n-k+2}\,...\sqrt{n}$.

4.5 Interpretation of Results

4.5.1 Initial Number State

Assume that the field state initially resides in a single number state $|n'\rangle$ and make use of the orthonormality property of number states, the corresponding wavefunction reduces to

$$|n'\rangle\langle n'|\Psi_I(t)\rangle = |n'\rangle\langle n'| \left(\sum_{n=0}^{\infty} c_{1,n}(t)\,|1\rangle|n\rangle + c_{2,n}(t)\,|2\rangle|n\rangle \right)$$
$$= c_{1,n}(t)\,|1\rangle|n'\rangle + c_{2,n}(t)\,|2\rangle|n'\rangle.$$

Hence the probability function for state 1 reduces to

$$P_1(t) = \left|c_{1,n}(t)\right|^2$$
$$= \cos^2\left(\frac{\Omega_R}{2}t\right) + \left(\frac{\Delta}{\Omega_R}\right)^2 \sin^2\left(\frac{\Omega_R}{2}t\right),$$

where $\Omega_R = \sqrt{\Delta^2 + 4\lambda^2 n'}$. It is therefore observed that the probability function simplified to the form derived in the semiclassical treatment (equation 4.27).

Moreover, the solution of two-photon model with initial number state actually reduces to the same form as above, with the exception that the constant n' is replaced with $\sqrt{n'-1}\sqrt{n'}$. In simple resonant case, such distinction only results in a minor difference in the angular frequency of the sinusoidal probability wave. Figure 4.3 illustrates the distinctions in probability graphs for one-photon model and two-photon model at $n' = 10$.

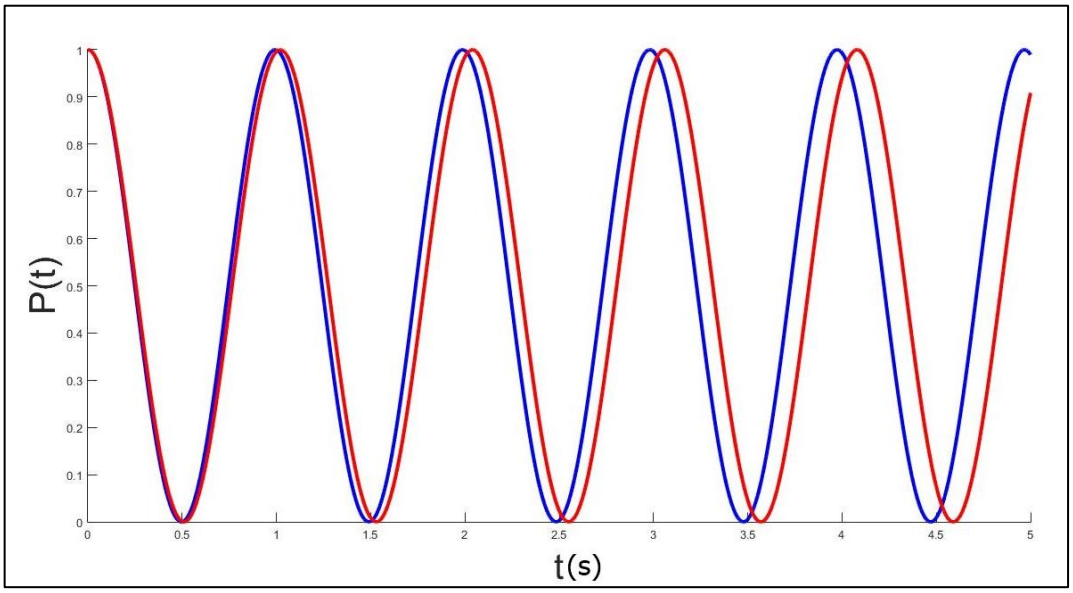

Figure 4.3: Probability graph to illustrate the comparison between single-photon model (blue) and two-photon model (red) with initial number state $n' = 10$.

4.5.2 Initial Coherent State (Single-Photon)

Assume that the field is initially in coherent state, the probability distribution function, as shown in equation 2.51 is

$$|a_n|^2 = \frac{\exp(-\bar{n})\,\bar{n}^n}{n!}.$$

In resonant case, the probability function for state 1 is

$$P_1(t) = \sum_{n=0}^{\infty} \left(\frac{\exp(-\bar{n})\,\bar{n}^n}{n!} \right) \cos^2\left(\lambda n^{1/2}\, t\right),$$

which is plotted using MATLAB software as shown from figures 4.4 to 4.7.

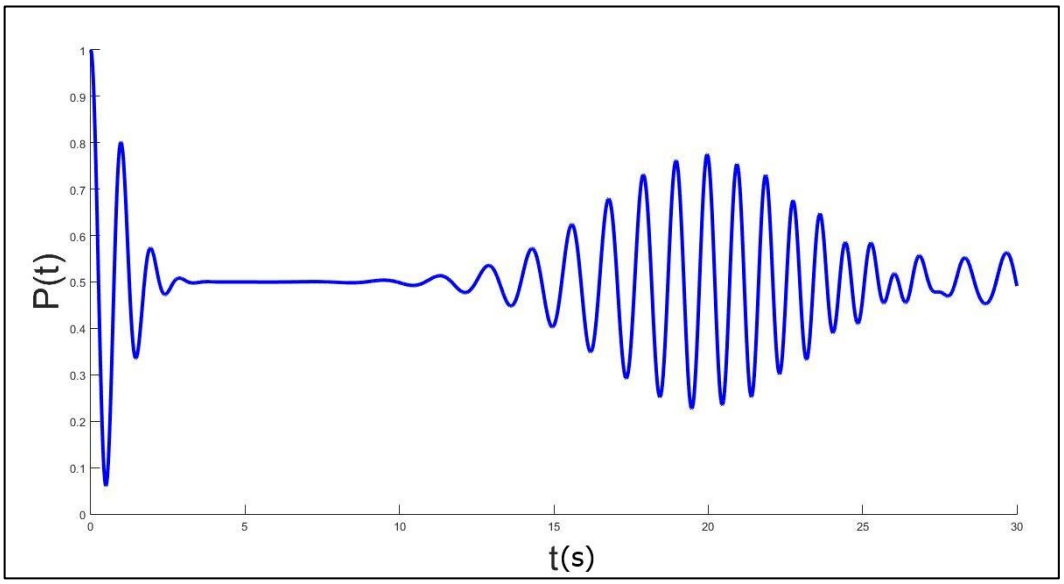

Figure 4.4: Probability graph of atomic ground state with initial coherent field state, mean photon number $\bar{n} = 10$ and interaction strength $\lambda = 1$.

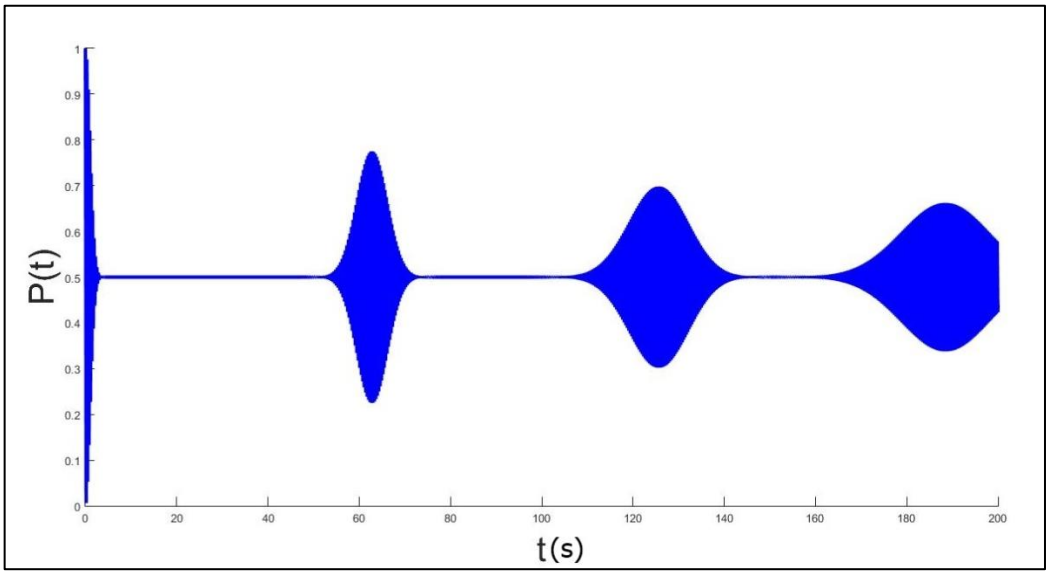

Figure 4.5: Probability graph of atomic ground state with initial coherent field state, mean photon number $\bar{n} = 100$ and interaction strength $\lambda = 1$.

Figures 4.4 and 4.5 show the probability function against time for the ground state of a two-level atom interacting with initial coherent photons. The mean photon number of the coherent field was set to $\bar{n} = 10$ (figure 4.4) and $\bar{n} = 100$ (figure 4.5) respectively. The probability function initially oscillates starting from a maximum value of $P(t) = 1$ which agrees with the assumption of initially unexcited atom. In figure 4.4 the oscillation amplitude gradually decreases until at approximately time

$t = 3\,s$, the oscillation ceases, resulting in a quiescence period at constant probability of 0.5. During this period the atom is in maximally mixed state, being equally likely to reside in either ground state or excited state. The Rabi oscillation however revives at around time $t = 13\,s$ with its amplitudes modulated in an envelope. The observation of collapse and revival of Rabi oscillation is unique in quantum mechanical treatment and serves as the direct evidence of the quantisation of photon fields. As time progresses, the feature becomes less prominent, the envelope that contains the revived Rabi oscillations becomes wider, and the envelope peaks decreases in amplitude.

Mathematically, the cause of the phenomenon of collapse and revival of Rabi oscillation is simply the destructive and constructive interference between individual *n*-th terms in the probability function. The type of interference exhibited by the total probability function depends on the phase-relation between the oscillating terms. If the oscillating terms are in-phase with each other, maximum constructive interference is observed; if the oscillating terms are anti-phase (π-phase difference) with each other, maximum destructive interference is observed.

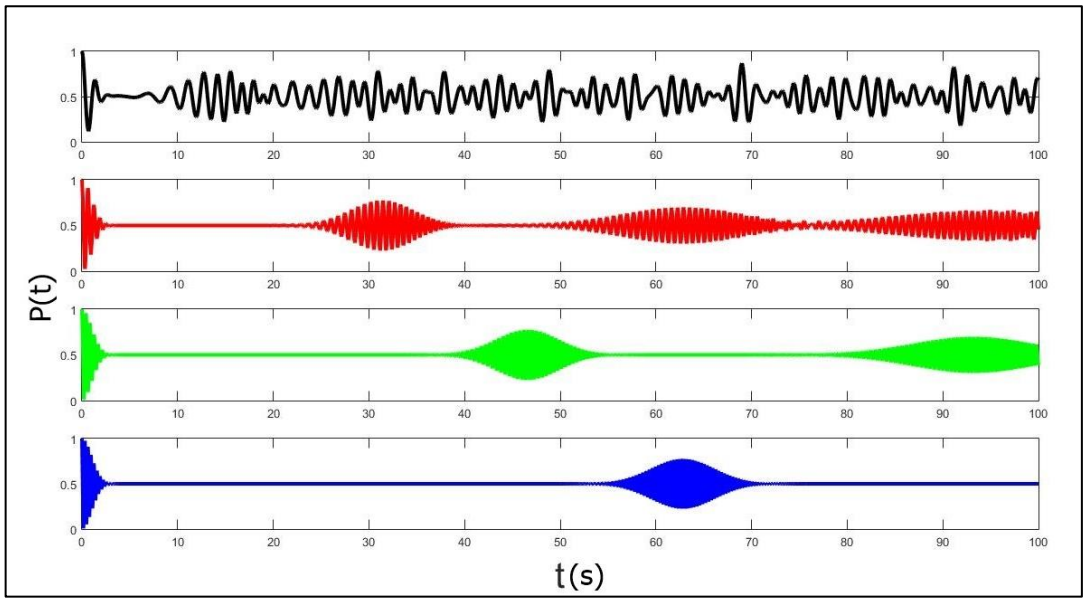

Figure 4.6: Probability graph of atomic ground state with initial coherent field state to illustrate the effects of mean photon numbers. From top to bottom: $\bar{n} = 5$ (black), $\bar{n} = 25$ (red), $\bar{n} = 55$ (green) and $\bar{n} = 100$ (blue).

Figure 4.6 illustrates the differences in the behaviour of the ground state probability function with various choices of mean photon number. At low mean photon number ($\bar{n} = 5$), little photon-atom interactions occur and hence the collapse and revival feature is not observed; instead the energy level of the atom oscillates between excited state and ground state in a chaotic manner. As the mean photon number increases, collapse and revival feature becomes more prominent. The frequency of the Rabi oscillation inside the envelopes also increases. On the contrary, higher mean photon number has very little, if any effect at all, on the average probability values. The quiescent periods remain at probability of 0.5 regardless of the mean photon number. Interestingly the period of time between revival features increases as the mean photon number increases, signifying that there may a relation between these two variables.

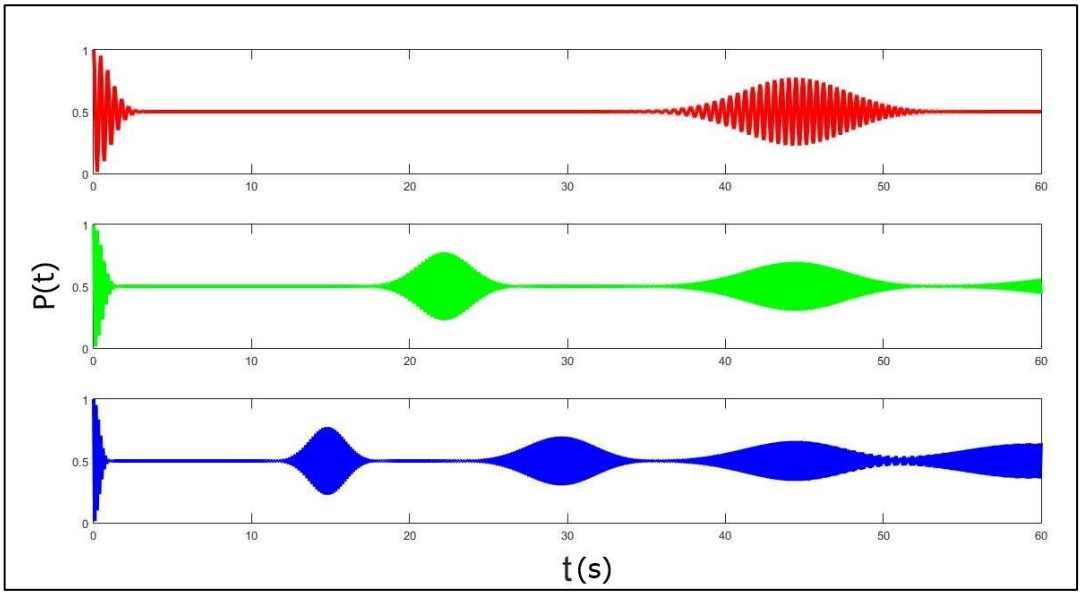

Figure 4.7: Probability graph of atomic ground state with initial coherent field state and $\bar{n} = 50$ to illustrate the effects of interaction strength λ. From top to bottom: $\lambda = 1$ (red), $\lambda = 2$ (green) and $\lambda = 3$ (blue).

Figure 4.7 displays the comparison between the ground state probability graphs with different interaction strengths. As its name suggests, the parameter λ measures the strength of interaction between the photons and the two-level atom. As the parameter increases, it is observed that the envelopes that contain the revived Rabi oscillations become increasingly narrower. Its width, however still becomes

wider as time progresses. The initial collapse of Rabi oscillation also happens sooner as the interaction strength increases. More importantly the period between revival features shortens with greater interaction strength, indicating some form of relations between these two parameters.

Since the observations from figures 4.6 and 4.7 indicate that the period between the revival features of Rabi oscillations is dependent on the mean photon number $\bar{n}$ and the interaction strength λ, it is therefore instructive to determine the exact relation between these variables which should be in the form of

$$T = f(\lambda, \bar{n}), \tag{4.69}$$

where T is the period between revival features.

First the interaction strength was set constant at value $\lambda = 1$ and the value of $\bar{n}$ was varied from 30 to 100. Through observation, the separation time between revival features is proportional to the square root of mean photon number $\bar{n}$. Hence the corresponding straight line graph is plotted as shown in figure 4.8. The corresponding raw data are shown in appendix A.

Similarly the mean photon number $\bar{n}$ was set constant at value $\bar{n} = 50$ and the value of λ was varied from 0.2 to 5.0. Through observation, the separation time between revival features is proportional to the inverse of the interaction strength λ. Thus the corresponding straight line graph is plotted in figure 4.9. The corresponding raw data are shown in appendix B.

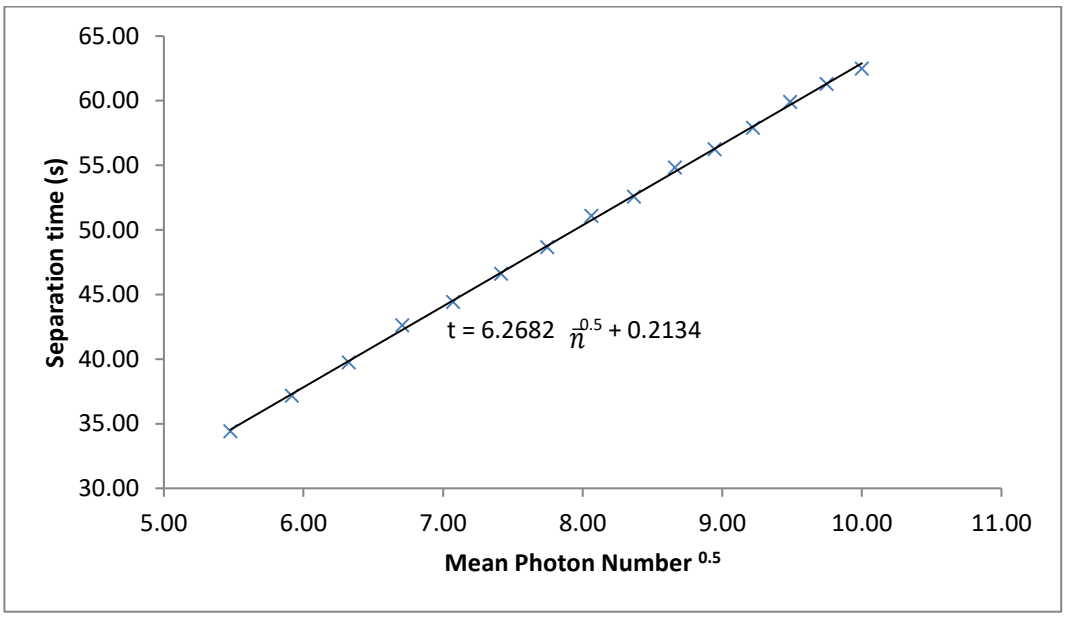

Figure 4.8: Graph of separation time between revival features against square root of mean photon number $\bar{n}$.

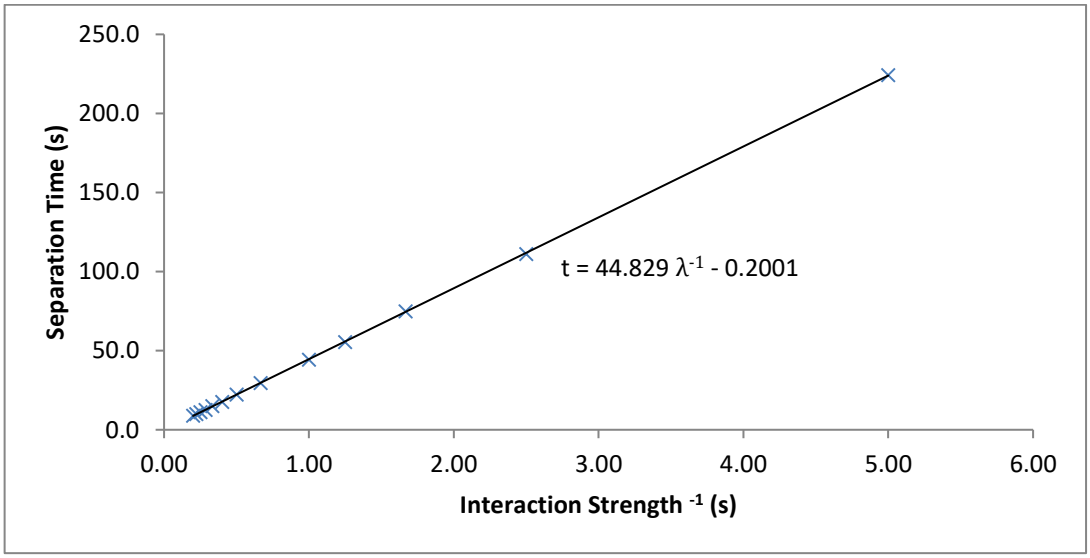

Figure 4.9: Graph of separation time between revival features against inverse of interaction strength λ.

From figure 4.8 and 4.9, it is easy to see that the formula in equation 4.69 may be simplified into

$$T = k\lambda^{-1}\sqrt{\bar{n}}, \tag{4.70}$$

where k is a constant. From figure 4.8, the straight line equation is approximately

$$T \approx 6.2682\sqrt{\bar{n}}.$$

Since $\lambda = 1$ in this case, hence the constant $k = 6.2682$. Similarly from figure 4.9, the straight line equation is approximately

$$T \approx 44.829\lambda^{-1}.$$

Since $\sqrt{\bar{n}} = \sqrt{50}$ in this case, hence the constant $k = 6.3398$. The average value is then $k = 6.3040$. Finally the expression 4.70 is found to be

$$T = 6.3040\ \lambda^{-1}\sqrt{\bar{n}},$$
$$T \approx 2\pi\ \lambda^{-1}\sqrt{\bar{n}}. \qquad (4.71)$$

On the other hand, in near resonant case the probability function for state 1 is

$$P_1(t) = \sum_{n=0}^{\infty}\left(\frac{\exp(-\bar{n})\,\bar{n}^n}{n!}\right)\left(\cos^2\left(\frac{\Omega_R}{2}t\right) + \left(\frac{\Delta}{\Omega_R}\right)^2 \sin^2\left(\frac{\Omega_R}{2}t\right)\right),$$

which is plotted using MATLAB software as shown in figure 4.10.

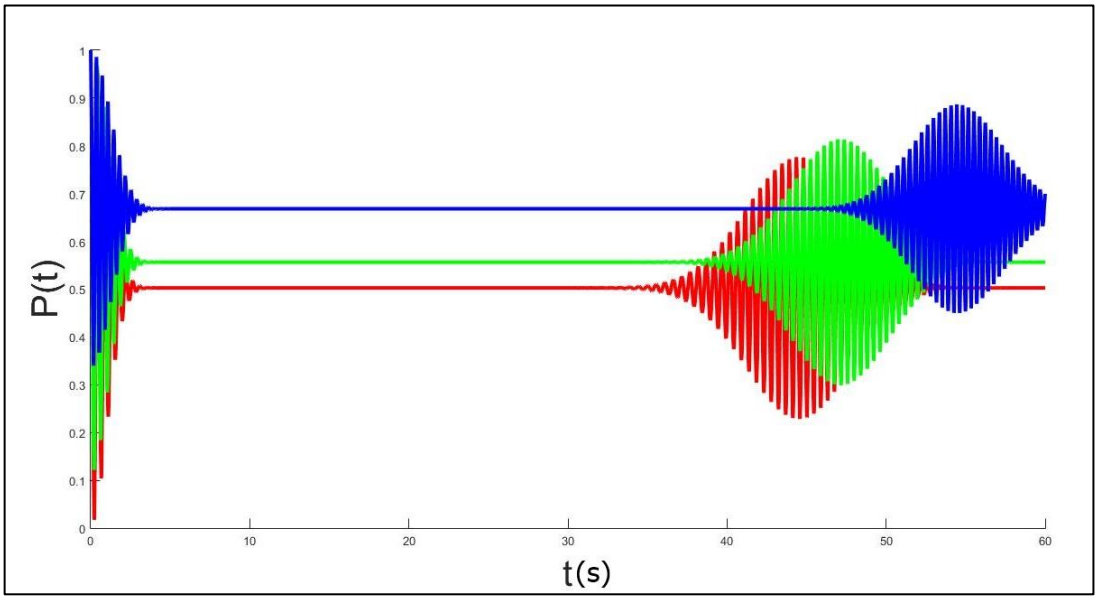

Figure 4.10: Probability graph of atomic ground state with initial coherent state and $\bar{n} = 50$ and different detuning. $\Delta = 1\ rad/s$ (red), $\Delta = 5\ rad/s$ (green) and $\Delta = 10\ rad/s$ (blue).

Figure 4.10 depicts the observations of the probability function with different values of detuning. Generally as the detuning increases, the atom has higher probability to reside in the ground state. This is expected because at higher detuning, the difference between photon energy and the energy gap of the two-level atom increases, causing the atom to be less likely to obtain sufficient energy from the photons and hence unable to jump into the excited state. Besides that, the quiescence period is also observed to increase with the detuning.

4.5.3 Initial Coherent State (Two-Photon)

The results of the coherent photon-atom interaction using two-photon model is shown and discussed in this section.

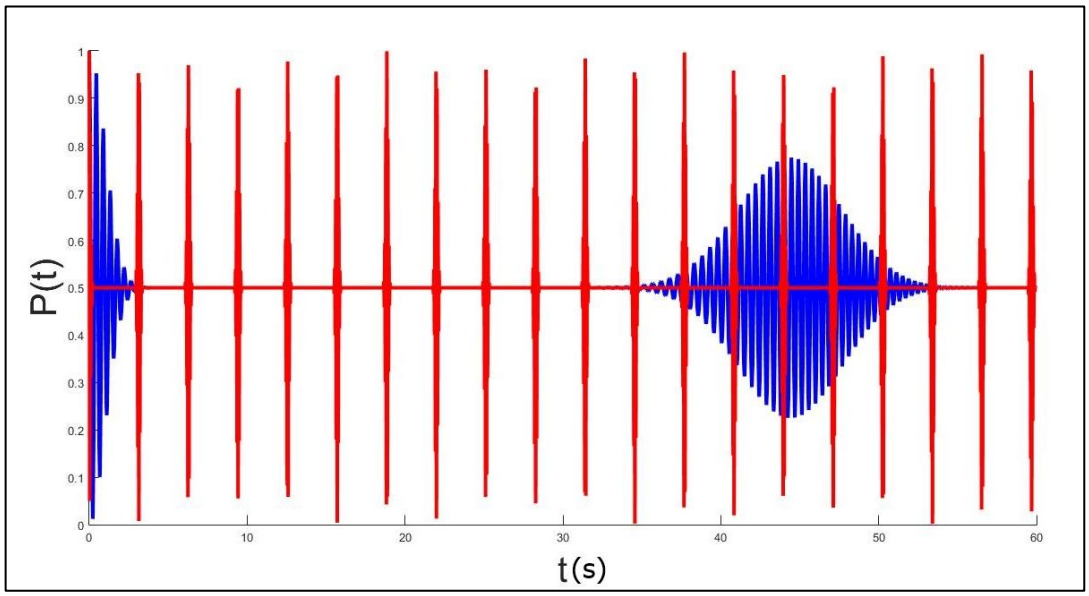

Figure 4.11: Probability graph of atomic ground state with initial coherent field state and mean photon number of $\bar{n} = 50$. The blue line represents single-photon model and the red line represents two-photon model.

Figure 4.11 illustrates the distinctions between one-photon model and two-photon model. One clear difference that can be observed is the period between revival features. The probability graph for two-photon model has significantly shorter time between revival features compared to one-photon model. The width of the envelope containing the Rabi oscillations is also much narrower for two-photon model compared to its one-photon counterpart. Furthermore, the peaks of revival of two-photon model are very high with values generally above 0.9, whereas one-photon model's peaks are only just above 0.7. Noticeably the quiescent periods, however remain the same at 0.5 probabilities for both one-photon model and two-photon model.

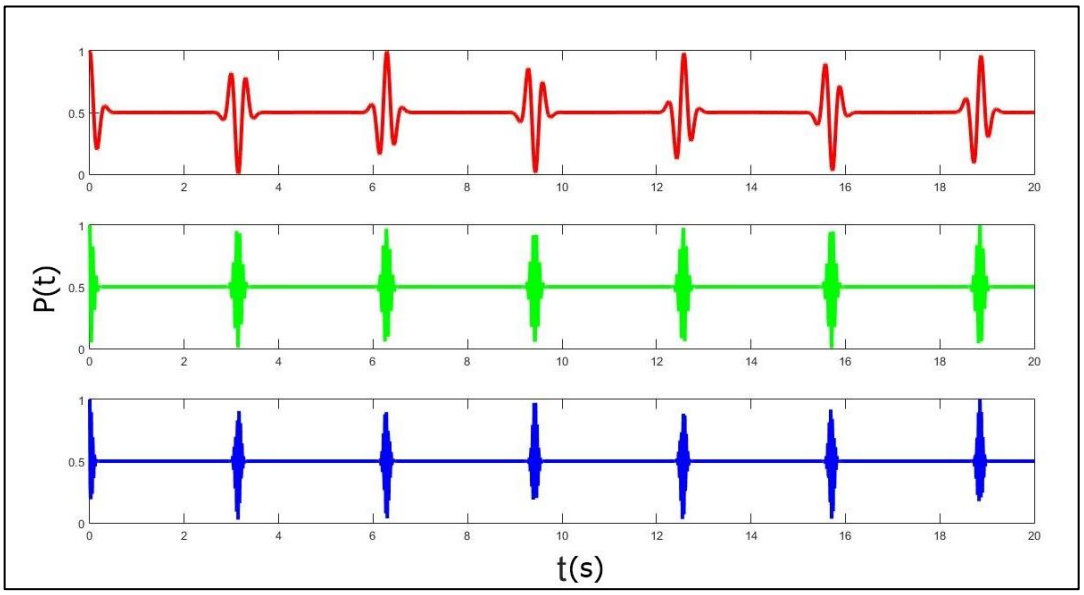

Figure 4.12: Probability graph of atomic ground state with initial coherent field state using two-photon model to illustrate the effects of mean photon numbers. From top to bottom: $\bar{n} = 10$ (red), $\bar{n} = 50$ (green) and $\bar{n} = 100$ (blue).

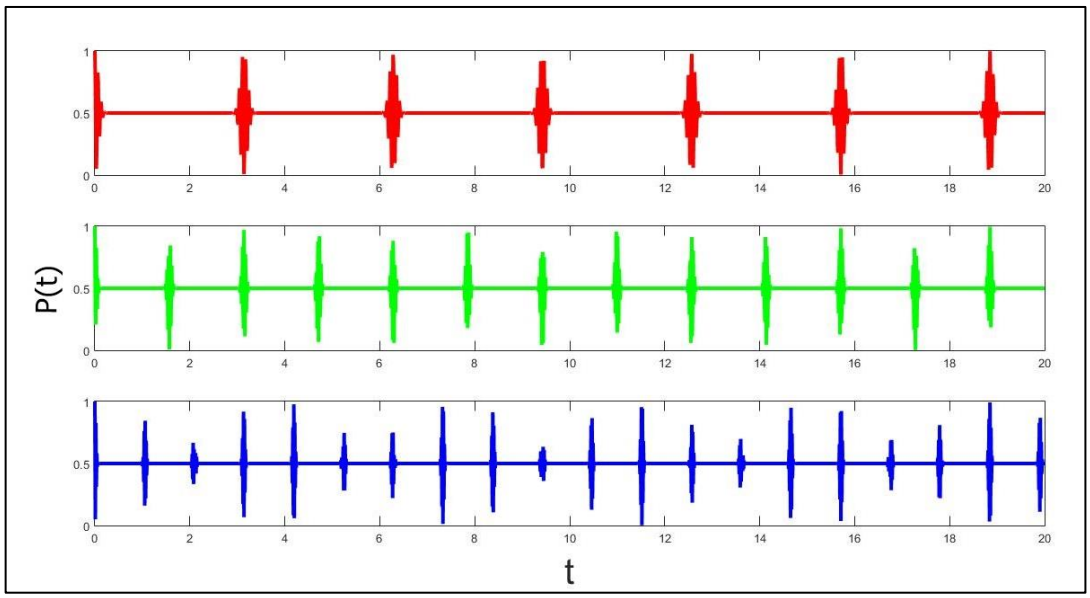

Figure 4.13: Probability graph of atomic ground state with initial coherent field state and $\bar{n} = 50$ using two-photon model to illustrate the effects of interaction strength λ. From top to bottom: $\lambda = 1$ (red), $\lambda = 2$ (green) and $\lambda = 3$ (blue).

Figure 4.12 reveals the comparison between two-photon models with different mean photon number. Generally there are little differences between the graphs. The collapse and revival features take place at pretty much the same time

with generally the same distribution of probabilities. A clear distinction however, can be made on the revived Rabi oscillations. Similar to the case in single-photon model, the frequency of the Rabi oscillations in the envelope increases with the mean photon number.

Figure 4.13 displays the comparison between two-photon models with different interaction strength. Interestingly as the interaction strength increases, more collapse and revival features can be observed within the same period of time. However at higher interaction strength, some of the revived Rabi oscillations have lower peaks at around 0.6 compared to other revival features which are usually above 0.8.

4.5.4 Initial Thermal State (Single-Photon)

Assume that the field is initially in thermal state, the probability distribution function, as shown in equation 2.55 is

$$|a_n|^2 = \frac{\bar{n}^n}{(\bar{n}+1)^{n+1}}.$$

In resonant case, the probability function for state 1 is

$$P_1(t) = \sum_{n=0}^{\infty} \left(\frac{\bar{n}^n}{(\bar{n}+1)^{n+1}}\right) \cos^2\left(\lambda n^{1/2}\, t\right),$$

which is plotted using MATLAB software as shown in figures 4.14, 4.15 and 4.16.

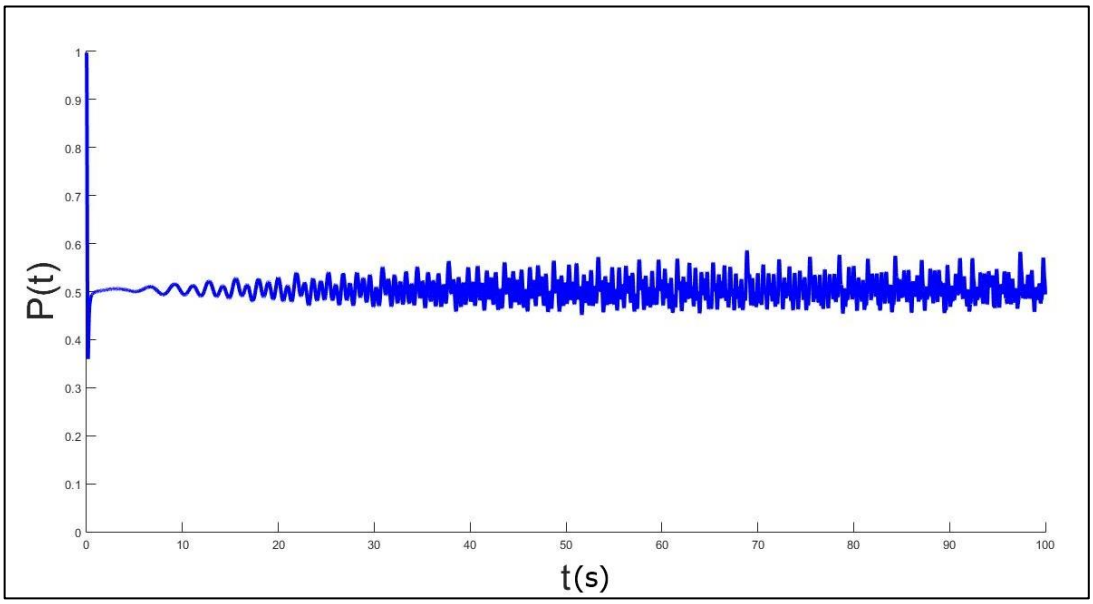

Figure 4.14: Probability graph of atomic ground state with initial thermal state, mean photon number $\bar{n} = 100$ and interaction strength $\lambda = 1$.

Figure 4.14 shows the probability function against time for the ground state of a two-level atom interacting with initial thermal photons. The mean photon number of the thermal field was set to $\bar{n} = 100$. Unlike the case in coherent field, no collapse and revival features of Rabi oscillations can be observed. The probability function fluctuates chaotically and no distinctive oscillation feature is observed even after a long time ($t = 100\ s$). The observation made from the initial thermal field is vastly different from the initial coherent field. The chaotic behaviour is attributed to the fact that thermal field is a statistical mixture with minimum amount of information other than its mean value of energy.

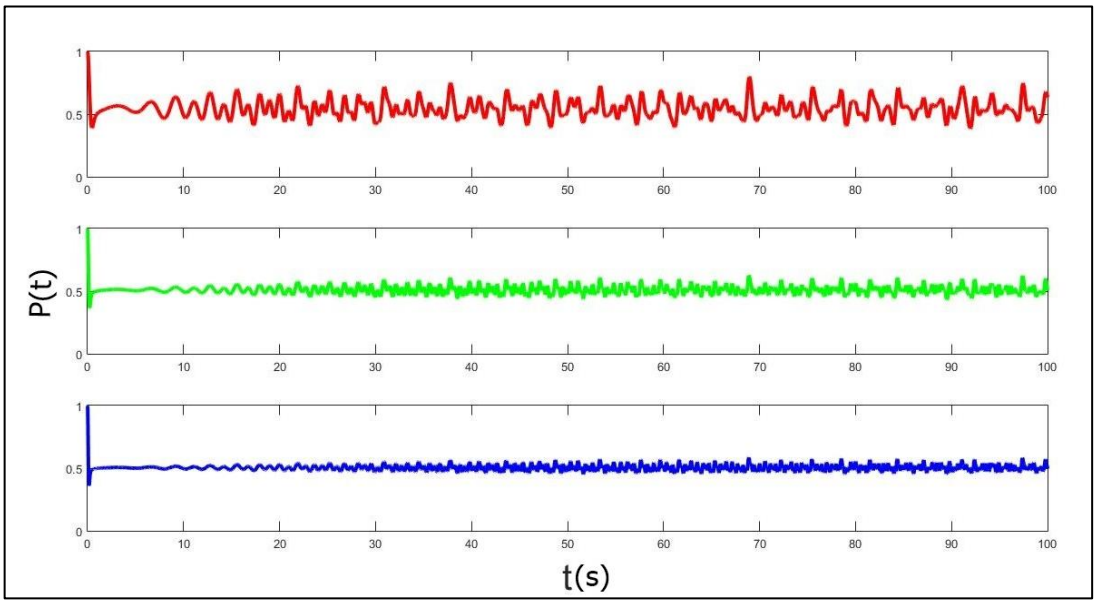

Figure 4.15: Probability graph of atomic ground state with initial thermal field state to illustrate the effects of mean photon numbers. From top to bottom: $\bar{n} = 10$ (red), $\bar{n} = 50$ (green) and $\bar{n} = 100$ (blue).

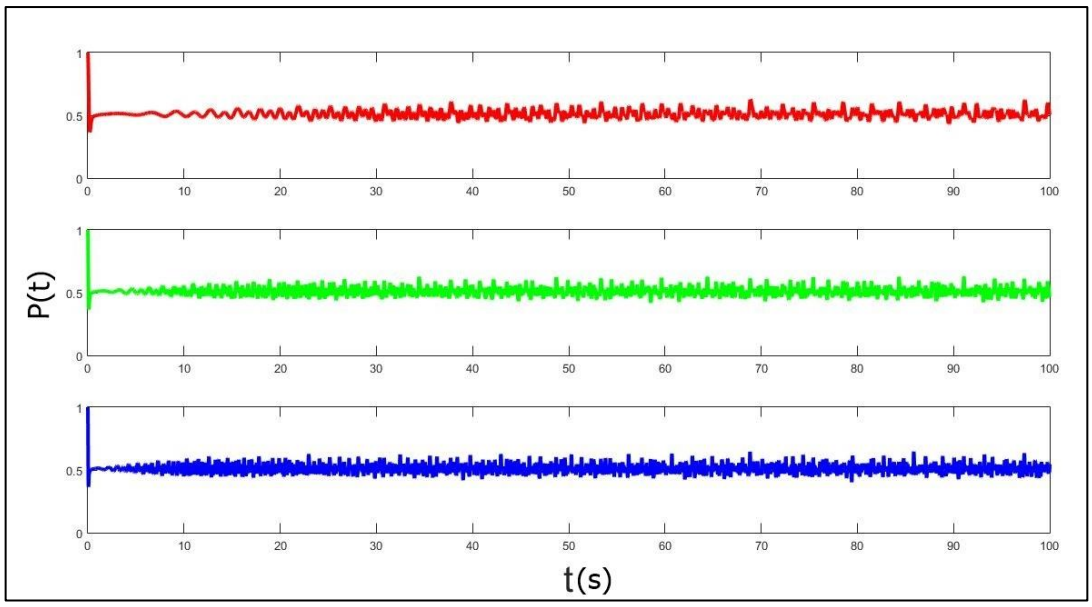

Figure 4.16: Probability graph of atomic ground state with initial thermal field state and $\bar{n} = 50$ to illustrate the effects of interaction strength λ. From top to bottom: $\lambda = 1$ (red), $\lambda = 2$ (green) and $\lambda = 3$ (blue).

Figure 4.15 illustrates the differences in the behaviour of the ground state probability functions with different mean photon numbers. The feature of chaotic fluctuation persists even with different mean photon number. It is observed that as

the mean photon number increases, the probability graphs have smaller fluctuations around the probability 0.5. Besides that, figure 4.16 shows no observable differences between the ground state probabilities of the atom with different interaction strength. In sum, the mean photon number and interaction strength parameters have little to no effect on the probability functions. The atom generally remains chaotic as it interacts with thermal photons.

In near resonant case, the probability function for state 1 is

$$P_1(t) = \sum_{n=0}^{\infty} \left(\frac{\bar{n}^n}{(\bar{n}+1)^{n+1}} \right) \left(\cos^2\left(\frac{\Omega_R}{2} t\right) + \left(\frac{\Delta}{\Omega_R}\right)^2 \sin^2\left(\frac{\Omega_R}{2} t\right) \right),$$

which is plotted using MATLAB software as shown in figure 4.17.

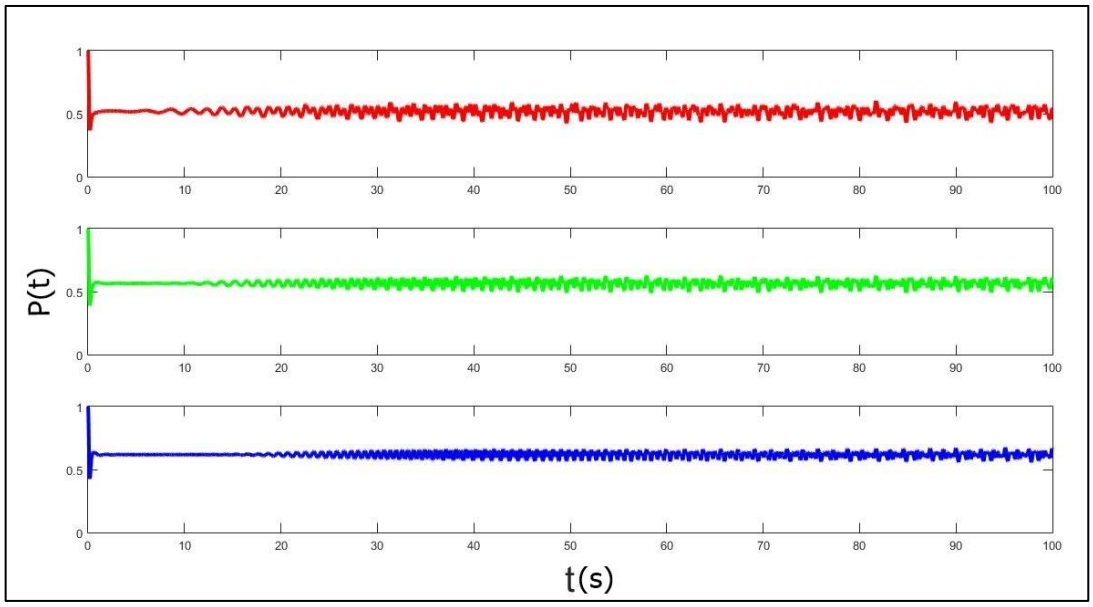

Figure 4.17: Probability graph of atomic ground state with initial thermal state and $\bar{n} = 10$ and different detuning. From top to bottom: $\Delta = 1\ rad/s$ (red), $\Delta = 5\ rad/s$ (green) and $\Delta = 10\ rad/s$ (blue).

Figure 4.17 depicts the observations of the probability function with different values of detuning. Similar to initial coherent state, as the detuning increases, the atom is more likely to be found in the ground state. Expectedly, the probability graphs of the ground state of the two-level atom remain chaotic as detuning increases.

With higher detuning, the amplitudes of the fluctuations also decrease, rendering the probability function to have greater resemblance to quiescence behaviour.

4.5.5 Initial Thermal State (Two-Photon)

The results of thermal photon-atom interaction using two-photon model is shown and discussed in this section.

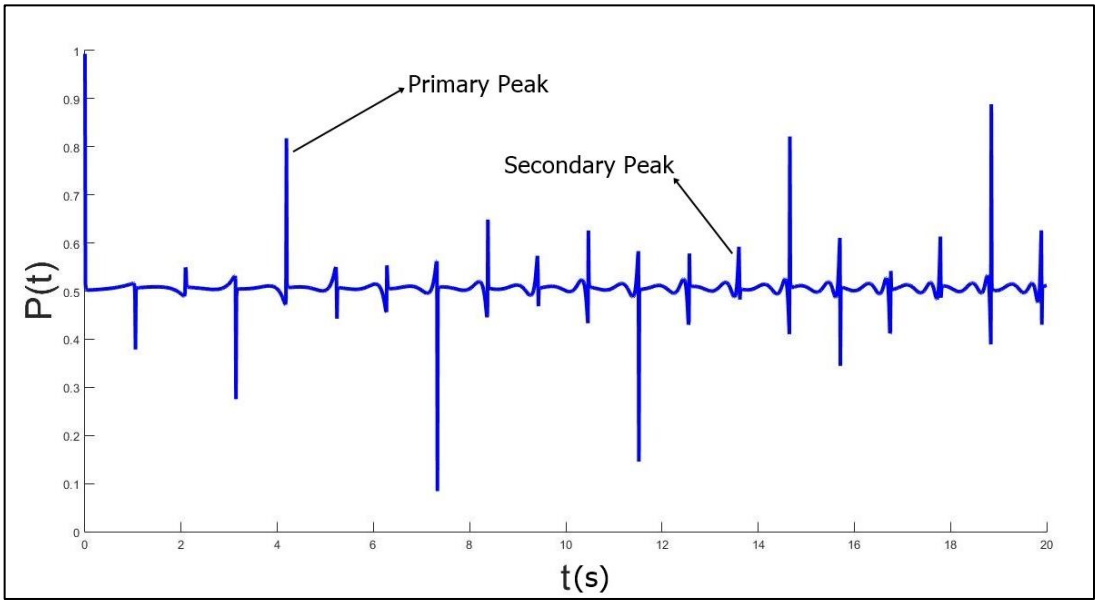

Figure 4.18: Probability graph of atomic ground state with initial thermal state using two-photon model and mean photon number of $\bar{n} = 100$ (shorter time range).

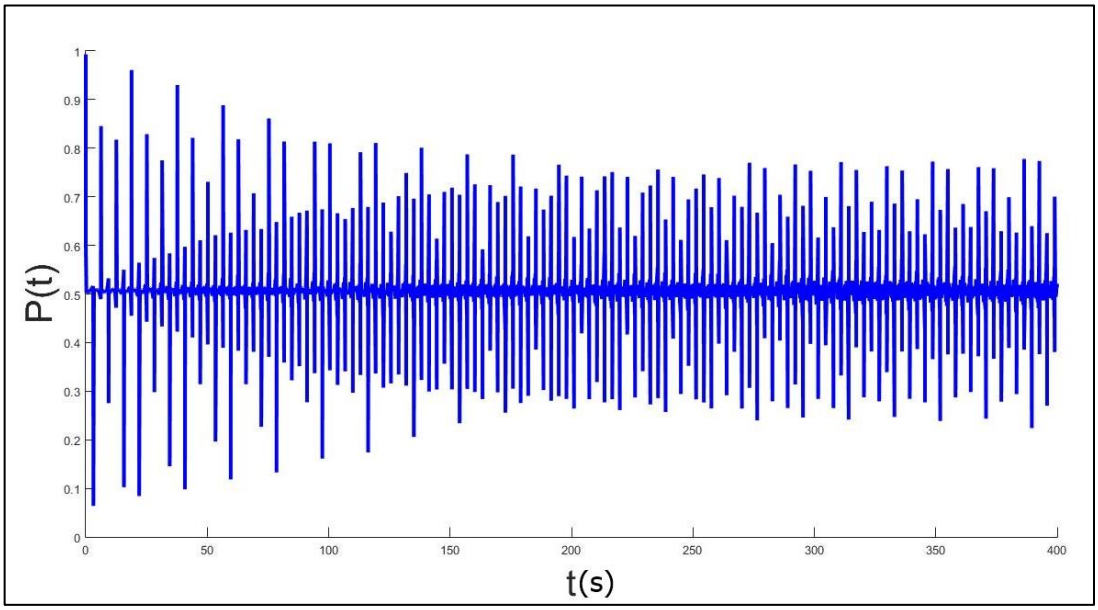

Figure 4.19: Probability graph of atomic ground state with initial thermal state using two-photon model and mean photon number of $\bar{n} = 100$ (longer time range).

Figures 4.18 and 4.19 illustrate the probability graphs of two-photon model using initial thermal state. While it is observed that the probability function is generally at 0.5, numerous sharp peaks can be observed as well. Suppose we categorise these peaks into two types: primary peak (higher amplitude) and secondary peaks (lower amplitude). While it is observed that primary peaks generally do not occur consecutively, the order between primary and secondary peaks remain seemingly random. Curiously the time between peaks is generally the same. However if the probability graph is viewed over a long time as shown in figure 4.19, it is observed that the secondary peaks slowly increase over time whereas the primary peaks gradually decrease over time. After a long time (around $150\ s$), the peaks transformed so much in amplitude that the two types of peaks can no longer be clearly differentiated, with the average probability centre around 0.5.

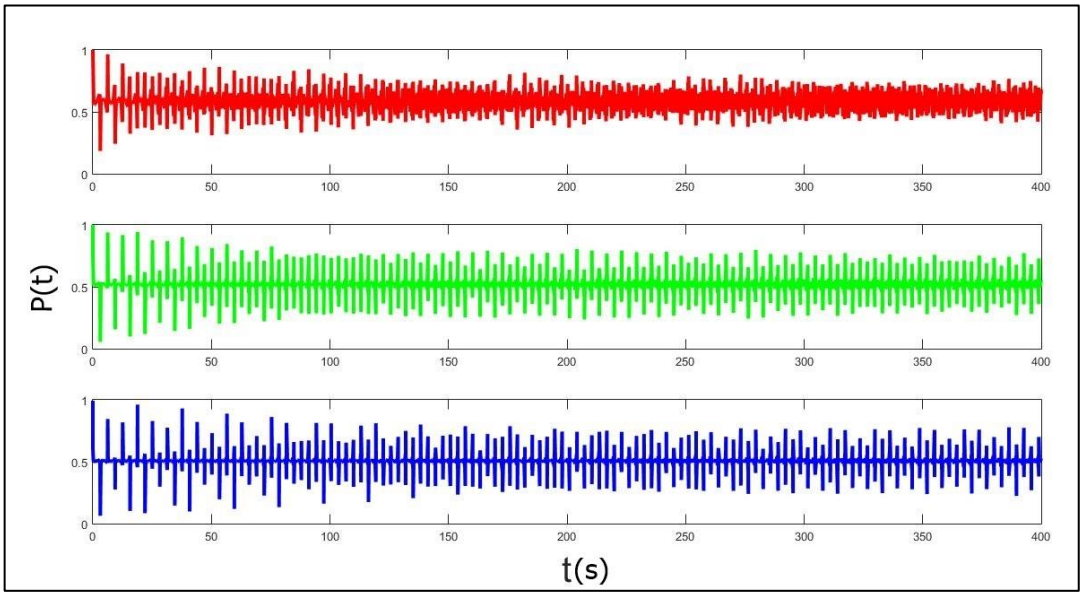

Figure 4.20: Probability graph of atomic ground state with initial thermal field state using two-photon model to illustrate the effects of mean photon numbers. From top to bottom: $\bar{n} = 10$ (red), $\bar{n} = 50$ (green) and $\bar{n} = 100$ (blue).

Figure 4.20 reveals the comparison between two-photon models with different mean photon numbers. Generally there are little differences between the graphs. The transformations of the primary and secondary peaks take longer time to be undifferentiated as the mean photon number increases. It is also observed that at lower mean photon number, the average probability shifts slightly upward. This may be caused by less possible interactions at lower mean photon numbers, therefore it is less likely that the two-level atom is to be excited.

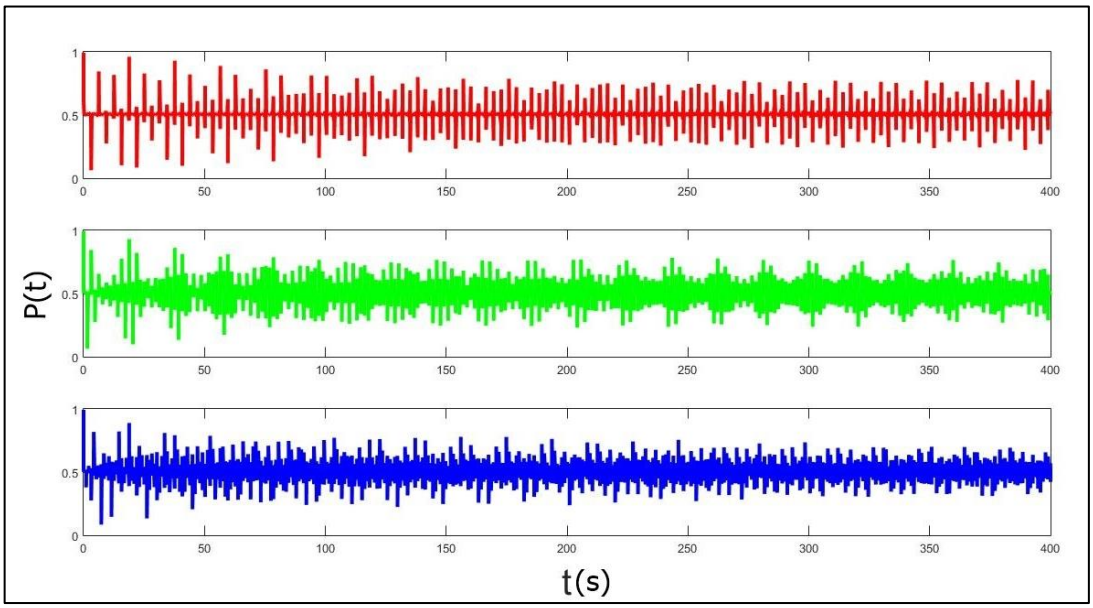

Figure 4.21: Probability graph of atomic ground state with initial thermal field state and $\bar{n} = 50$ using two-photon model to illustrate the effects of interaction strength λ. From top to bottom: $\lambda = 1$ (red), $\lambda = 2$ (green) and $\lambda = 3$ (blue).

Figure 4.21 displays the comparison between two-photon models with different interaction strength. With stronger interaction strength, the transformation of the primary and secondary peaks takes much shorter time to become undifferentiated. In fact, the distinctions between the two peaks become less prominent as interaction strength increases. This is in-line with the understanding of thermal interaction with atom. As interaction strength increases, thermal photons are interacting more strongly with the two-level atom, resulting in the atom gaining more of the chaotic nature. Hence the distinctions lessen and the probability graph becomes more randomised.

CHAPTER 5

CONCLUSIONS AND RECOMMENDATIONS

5.1 Conclusions

In semiclassical treatment, the interaction between a single-mode classical field and a quantum mechanical two-level atom is studied. The probability of the atom to be in the ground state and excited state are derived to be $P_1(t) = \cos^2 \frac{1}{2}\Omega t$ and $P_2(t) = \sin^2 \frac{1}{2}\Omega t$ respectively, where Ω is the Rabi frequency. Dipole approximation and rotating-wave approximation are utilised in the derivation process. It is found that the populations in the ground state and the excited state oscillate with Ωt. Two cases of detuning are investigated: exact resonance and near resonance. In exact resonance, the conservation of probability holds for both the ground state and the excited state; whereas in near resonance, the conservation is no longer valid and it is found that the period and the amplitude decreases with increasing detuning.

In full quantum mechanical treatment, the interaction between a single-mode quantised light-field of various field states and a quantum mechanical two-level atom is studied. The probability of the atom to be in the ground state is derived to be $P_1(t) = \sum_{n=0}^{\infty} |a_n|^2 \left(\cos^2 \left(\frac{\Omega_R}{2} t \right) + \left(\frac{\Delta}{\Omega_R} \right)^2 \sin^2 \left(\frac{\Omega_R}{2} t \right) \right)$, where Ω_R is the Rabi frequency and a_n is the probability distribution of the initial field state. Rotating wave approximation was used in the derivation process.

The effects of parameters such as interaction strength, mean photon number and detuning on the ground state probability functions are studied. When number state is assumed to be the initial field state, the probability function reduces to the similar form as semiclassical treatment, exhibiting uniform oscillation behaviour. On the other hand, initial thermal state renders the probability function of the two-level atom to be generally chaotic. Most interestingly, imposing initial coherent state condition returns the result of collapse and revival feature of Rabi oscillations which is a signature of quantised light field. The same observation cannot be obtained using classical treatment of light-matter interaction. Besides that, the model was also extended from one-photon model to two-photon model. Generally the trends of the probability graphs in two-photon model are mostly similar as in single-photon case.

5.2 Recommendations for future work

In this study, we used rotating-wave approximation in both semiclassical and quantum mechanical treatments to simplify the expressions in the derivation process. Such approximation is justified by the fact that fast rotation terms may be averaged to zero, thus these terms will have little effects on the expression containing it. Nonetheless, derivation process without the usage of rotating-wave approximation may be attempted in future work to obtain a more complete picture of the final expression.

Moreover, this study focused solely on a closed two-level system. This study may therefore be extended to investigate a system with more energy levels (e.g. three-level system). To further align with practical purposes, this study may also be extended to open systems where energy dissipation and quantum decoherence may occur. Then, a generalisation of quantum mechanical interaction between photon and atom may be performed based on these results.

REFERENCES

Barnett, S. M. and Radmore P. M., 1997. *Methods in Theoretical Quantum Optics*. New York: Oxford University Press.

Dick, R., 2016. Analytic sources of inequivalence of the velocity gauge and length gauge. *Physical Review A*, 94(6), pp. 062118.

Griffiths, D. J., 1994. *Introduction to Quantum Mechanics*. London: Prentice-Hall International Limited.

Griffiths, D. J., 1999. *Introduction to Electrodynamics*. New Jersey: Prentice Hall.

Han, Y. C. and Madsen L. B., 2010. Comparison between length and velocity gauges in quantum simulations of high-order harmonic generation. *Physical Review A*, 81(6), pp. 063430.

Loudon, R., 2000. *The Quantum Theory of Light*. 3rd ed. New York: Oxford University Press Inc.

Phoenix, S. J. D. and Knight, P. L., 1990. Periodicity, phase, and entropy in models of two-photon resonance. *Journal of Optical Society America B*, 7(1), pp. 116-124.

Rzazewski, K. and Boyd, R. W., 2004. Equivalence of interaction Hamiltonians in the electric dipole approximation. *Journal of Modern Optics*, 51(8), pp. 1137-1147.

Schleich, W. P., 2001. *Quantum Optics in Phase Space*. Berlin: WILEY-VCH.

Shafer, R. T., 2009. *Three Pictures of Quantum Mechanics*. [lecture note] Available at: http://uncw.edu/phy/documents/Shafer_09.pdf [Accessed 30 May 2017].

Steck, D. A., 2007. *Quantum and Atom Optics*. 1st ed. [ebook] Available at: http://steck.us/teaching/ [Accessed 1 Mar. 2017].

Sukumar, C. V. and Buck, B., 1981. Multi-Photon Generalisation of the Jaynes-Cummings Model. *Physics Letters*, 83A(5), pp. 211-213.

APPENDICES

APPENDIX A: Data for Figure 4.8

Table A.1: Data for Graph in Figure 4.8.

Mean Photon Number, $\bar{n}$	$\sqrt{\bar{n}}$	**Separation Time, T (s)**
30	5.48	34.43
35	5.92	37.18
40	6.32	39.74
45	6.71	42.62
50	7.07	44.44
55	7.42	46.60
60	7.75	48.67
65	8.06	51.10
70	8.37	52.58
75	8.66	54.83
80	8.94	56.24
85	9.22	57.91
90	9.49	59.92
95	9.75	61.29
100	10.00	62.48

APPENDIX B: Data for Figure 4.9

Table B.2: Data for Graph in Figure 4.9

Interaction Strength, λ (s^{-1})	**λ^{-1} (s)**	**Separation Time, T (s)**
0.2	5.00	224.3
0.4	2.50	111.1
0.6	1.67	74.9
0.8	1.25	55.6
1.0	1.00	44.4
1.5	0.67	29.6
2.0	0.50	22.2
2.5	0.40	17.6
3.0	0.33	15.0
3.5	0.29	12.6
4.0	0.25	11.1
4.5	0.22	10.0
5.0	0.20	9.0